Chapter II:
Surface structure of westerly wind events.

II.1. Introduction

In this chapter I explore the spatial and temporal characteristics of westerly wind events (WWEs) over the Western and Central Tropical Pacific Ocean, from 1986 through 1995. This work has been described in Harrison and Vecchi (1997), with Vecchi and Harrison (1997) serving as a complementary Technical Memorandum containing a comprehensive set of figures and tables which detail all the results. The results outlined here are the first rigorous statistical analysis of the 3-D space-time evolution of WWEs. These results, especially the WWE classification and definition scheme, are the main foundation upon which the rest of the work described in this Dissertation builds.

WWEs are a dominant mode of the sub-seasonal surface wind variability over the tropical Pacific Ocean (Luther *et al.* 1983, Harrison and Luther 1990) characterized by large amplitude (10-20 ms^{-1}), short timescale (6-20 day) westerly wind anomalies in a system where the main surface wind anomalies are weak easterlies throughout most of the time (ie. the distribution of surface wind anomaly is skewed). There have been detailed descriptions of the evolution of the wind fields during individual WWE periods (*e.g.* Keen 1982, Love 1985a, Eldin *et al*. 1994, Chen and Houze 1995, Lin and Johnson 1996), however it is important to develop a view of the mean characteristics of WWEs for any general discussion. Harrison and Giese (1991) used 30 years of near-dateline island wind data to develop a description of the meridional-time structure of WWEs which occur near the dateline. Due to the limited zonal extent of the islands, Harrison and Giese (1991) were unable to describe the zonal scales of the WWEs, nor determine whether these WWEs exhibited zonal translation during their lifetime. Hartten (1996) used the U.S. Navy NOGAPS operational surface wind product to described the surface wind characteristics of west-of-dateline westerly wind

bursts. Hartten (1996) developed a subjective classification scheme for westerly wind bursts based on the circulation patterns of the westerly wind bursts; 90% of the westerly wind bursts in the period 1985-1994 fit into the 9 categories. However, the subjective nature of the classification scheme did not lend itself to rigorous statistical analysis of the data. It has been noted that there is a significant tendency for near-Dateline WWEs to be associated preferentially with warm El Niño-Southern Oscillation (ENSO) periods and with particular seasons (Luther *et al.* 1983, Harrison and Giese 1991, Hartten 1996).

The purpose of this work was to use the European Centre for Medium Range Weather Forecasts (ECMWF) operational surface wind analysis for the years 1986-1995 to develop a 3-D (latitude, longitude and time) characterization of WWEs. Since the early-1980s, the operational surface wind analysis product of the ECMWF has improved considerably; after extensive analysis of the ECMWF data I consider it to be plausible enough after 1986 to use as my surface wind dataset. Using the global gridded ECMWF operational wind data, the structure and existence of WWEs beyond the dateline could be explored, and tendencies for WWEs to translate could be determined.

I determined that it was possible to classify the WWEs into eight types based on the location of the maximum zonal wind anomalies of the WWEs. Using this classification scheme, an unambiguous WWE definition was developed, and intensity measures defined. Using the WWEs identified in the record, the composite surface wind fields were evaluated for each type of WWE. Using the composite wind fields as a guide, I developed a simple analytical model to further summarize the basic properties of each type of event. The TOGA-COARE Intensive Observation Period (November 1992 through February 1993) was used to test the applicability of the composite model to individual wind events. Finally, the temporal distribution was studied on monthly and inter-annual time scales of both the frequency and intensity of the WWEs.

In the following sections I describe the main results of the analysis of the surface

wind strunture of WWEs for the period 1986-1995. Section II.2 describes the data sets used; Section II.3 describes the classification scheme and the compositing technique used in this study. The composite results are presented and a simple mathematical model structure for these composite WWEs is described in Section II.4. The westerly wind variability during the TOGA-COARE Intense Observation Period and the ability of the composite events to characterize the IOP variability is presented in Section II.5. Section II.6 discusses the seasonal and inter-annual distribution of WWEs and their correlation with the Southern Oscillation Index, and describes the extent to which WWEs occur in particular sequences. Section II.7 offers some summary and discussion.

I.2. Data

The wind data set used is the ECMWF 10-m operational 12 hourly wind analysis, on their 2.5°x2.5°global grid. Attention was on the region from 100°E to 100°W, by 30°S to 30°N and over the years 1986-1995. The ECMWF analysis was significantly improved in the middle 1980s, hence the choice of 1986 for the beginning of this analysis effort. A monthly climatology was constructed from the 12-hourly ECMWF surface wind analysis of the entire ten years of record (1986-1995), using a time axis centered on the mid-day of each month. Anomalies were defined as the difference between the instantaneous wind and the climatology, linearly interpolated in time.

In order to assess the utility of the ECMWF 10m wind field, two comparisons were carried out. First the large time and space scale aspects of the circulation were determined by comparing the ECMWF monthly climatology to the COADS monthly climatology of ship observations from 1946 through 1993 (Woodruff *et al.* 1987). Then, to examine the short time scale variability, ECMWF time series is compared with data from the TOGA-TAO buoys (McPhaden 1993).

To summarize the results of comparing the ECMWF climatology with the COADS

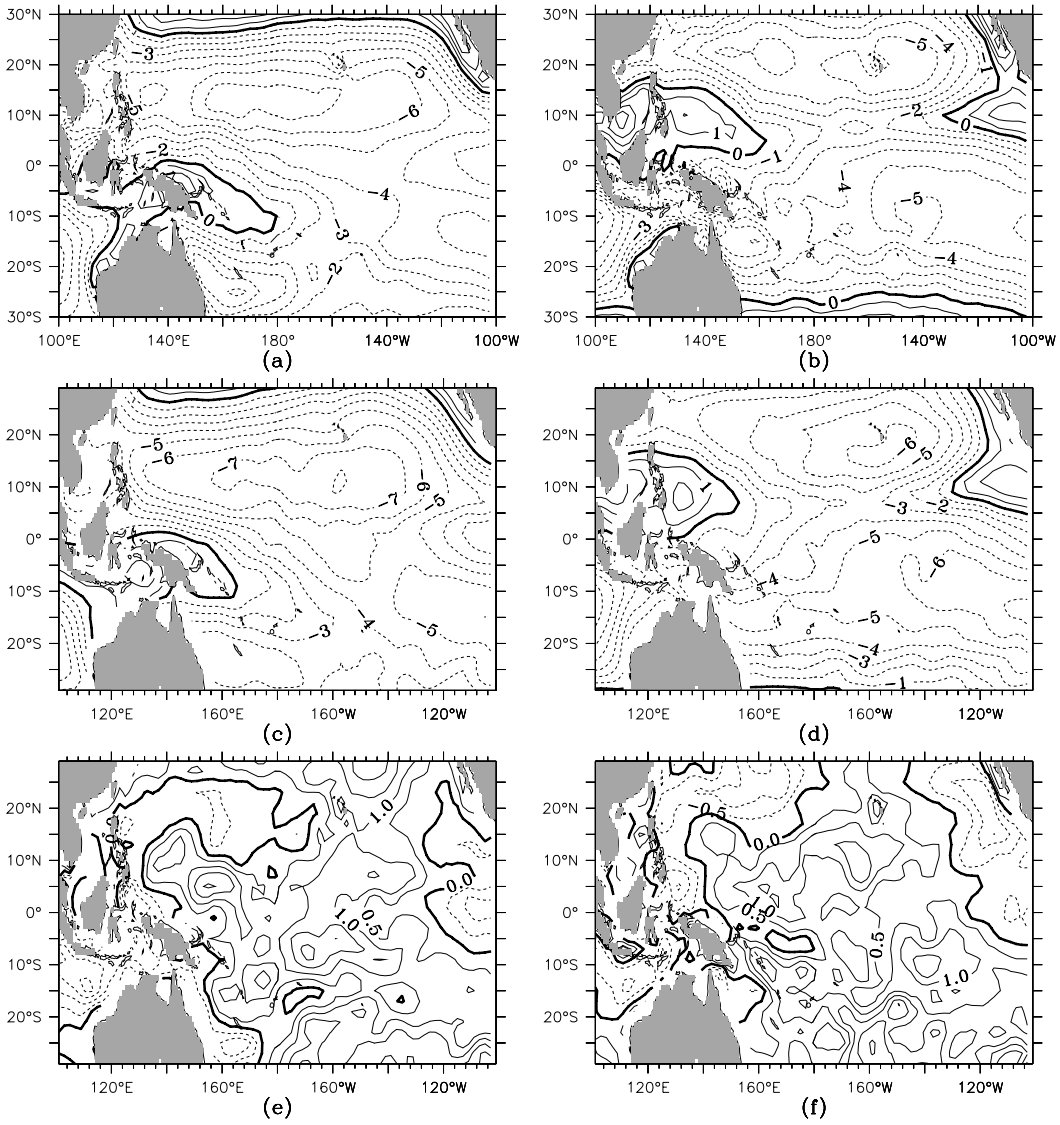

Figure II.1. Contours of (a) March and (b) September 10-m climatological zonal wind from ECMWF (1986-1995), (c) March and (d) September 10-m climatological zonal wind from COADS (1946-93), and (e) March and (f) September difference (ECMWF-COADS) 10-m climatological zonal wind. Dashed contours indicate negative values. COADS climatology data is smoothed using a five-point triangle filter in the zonal direction and a three-point triangle filter in the meridional direction. Contour interval is 1.0 ms^{-1} for (a)-(d), and 0.5 ms^{-1} for (e)-(f).

climatology, the wind data are shown for March and September (Figures II.1-.3). Contour plots are shown for the ECMWF climatology from 1986 through 1995, for the COADS climatology from 1946 through 1993 and for the difference ECMWF - COADS, for zonal wind (Figure II.1), meridional wind (Figure II.2) and wind divergence (Figure II.3). For all these plots the COADS climatology is smoothed with a 5-point triangle filter (half power

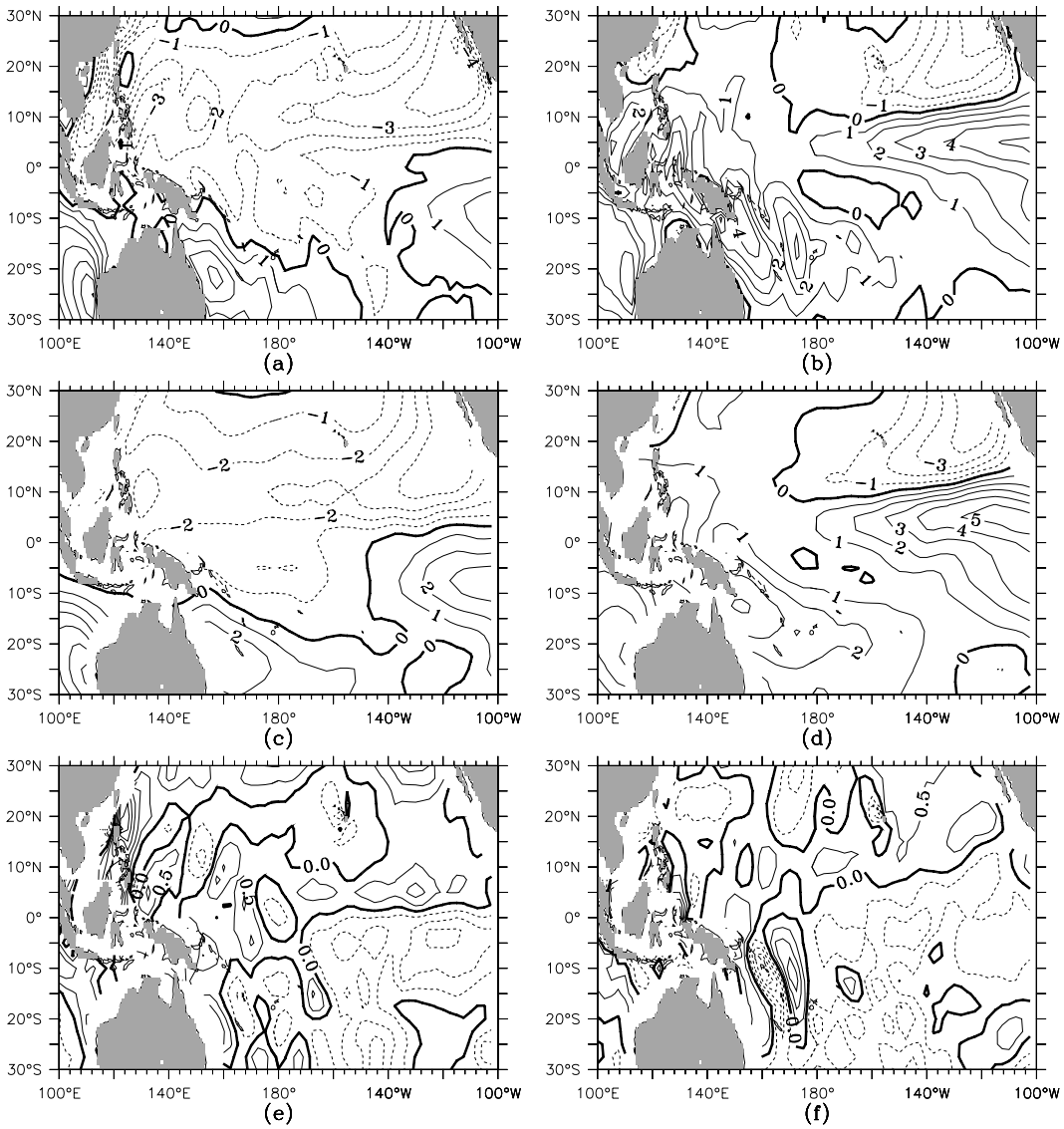

Figure II.2. Same as Figure 1, except for 10-m meridional wind.

point at 18°) in the zonal direction and a 3-point triangle smoother (half power point at 11°) in the meridional direction.

The ECMWF climatology reproduces the main aspects of the large scale circulation appropriately (Figures II.1, .2). The zonal wind cores of the SE and NE trade winds are clear in Figure II.1, and their magnitudes are comparable to the ship-based winds of COADS. The small area of western Pacific equatorial westerlies in March, and the comparable band of westerlies from SE Asia to 160°W along 10°N in September are present in the ECMWF

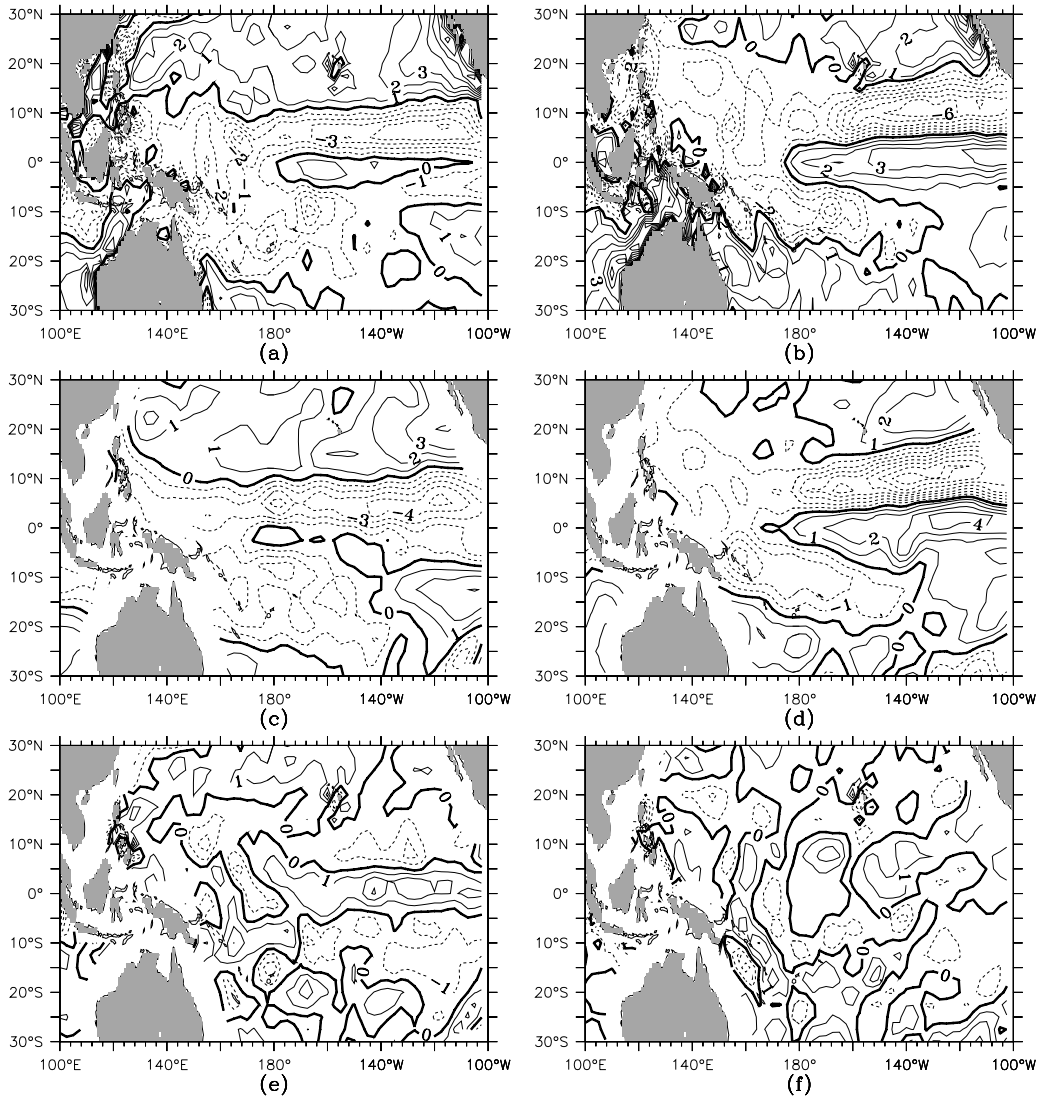

Figure II.3. Same as Figure 1, except for 10-m wind divergence. Contour interval is 10^{-6} s.

fields. The difference fields of zonal wind (Figure II.1-e,f) show considerable spatial structure, but the large scale difference is seldom more than 1.5ms^{-1} and is typically closer to 1ms^{-1}. Near the equator ECMWF winds tend to be weaker (less easterly) than the COADS winds west of 120°W and stronger (more easterly) east of 120°W. The SE trades tend to be weaker (less easterly) in ECMWF, but the NE trades are some places weaker and others stronger in ECMWF. The meridional wind comparisons of Figure II.2 also show considerable large scale similarity. The strong seasonal variations between 10°S and 15°N east of

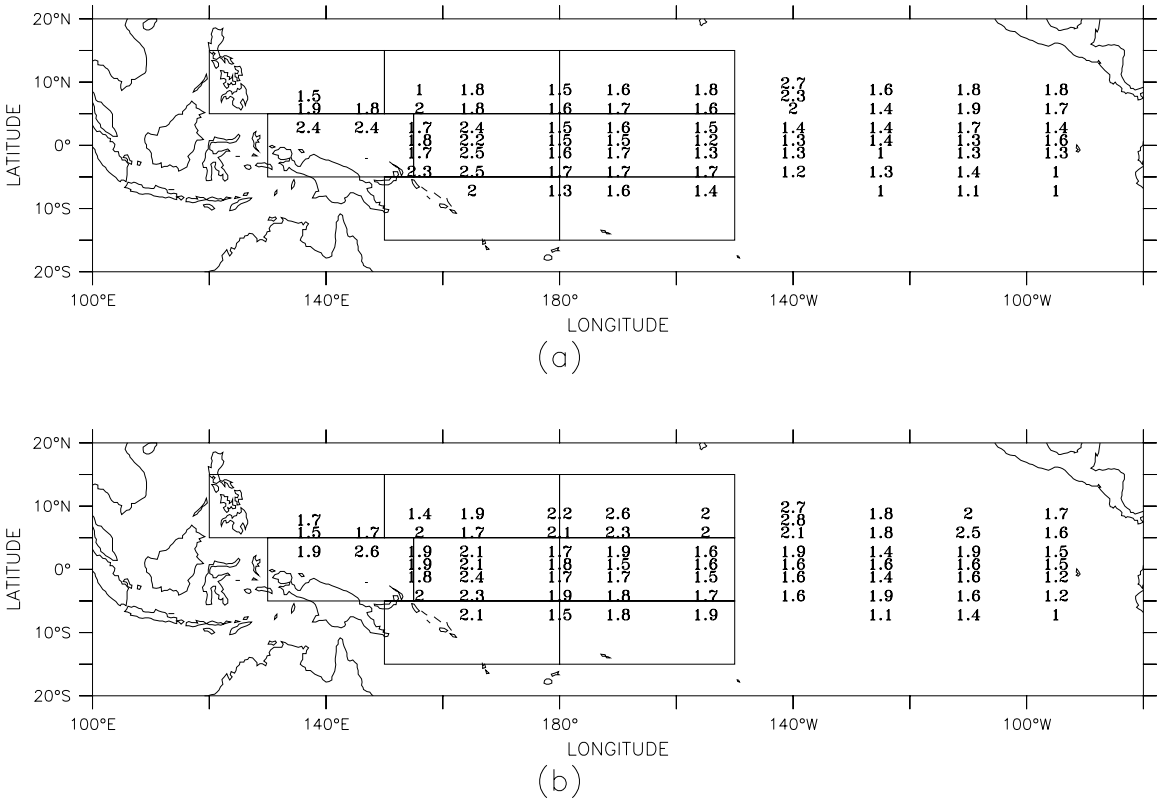

Figure II.4. Values of the rms difference (TAO-ECMWF) at selected TAO buoy locations for daily (a) surface zonal wind and (b) surface meridional wind. Units are ms^{-1}. The time period over which TAO data are available varies for each buoy. Supperimposed are the outlines of the WWE classifying regions.

the Dateline are well reproduced, as is the broad area of southerly wind east of Australia. However, there is much small space scale structure in ECMWF in the western tropical Pacific that has no counterpart in the COADS climatology. This is particularly evident in the meridional wind difference results (Figure II.2-e,f). The large scale meridional wind differences are typically less than $1ms^{-1}$, but NE of Australia they can exceed $1.5ms^{-1}$. The ECMWF climatology in general overestimates the meridional wind speed north of the Inter Tropical Convergence Zone (ITCZ) and underestimates it to the south, compared to COADS.

It is possible that the generally weaker near-equatorial easterlies in ECMWF result from their being a recent average, over a period in which ENSO conditions have been prominent. I have not pursued this possibility, because I judge the differences found here to be small enough to be of little concern for the topic of interest. WWEs typically have peak

zonal wind anomalies in excess of 10 ms^{-1} over a large area, so a 2 ms^{-1} difference is does not significantly affect the analysis or its main conclusions.

Another measure of the large scale aspects of the ECMWF analysis is the monthly mean divergence field. The March and September divergence patterns for the ECMWF and COADS climatologies are compared in Figure II.3. The two climatologies have similar divergence patterns, with maximum convergence in the ITCZ and the South Pacific Convergence Zone (SPCZ). Generally the location and meridional scale of each convergence zone are similar, but the ECMWF convergence is substantially weaker than COADS. The divergence patterns along the equator are rather different in March, with ECMWF indicating a clear band of divergence from the Dateline to about 110°W, but with COADS indicating a broad area of weak equatorial convergence east of 140°W. There are no large scale differences in the central and western tropical Pacific sufficient to merit concern.

The RMS difference between the daily averaged ECMWF wind analysis, interpolated to each buoy location (when necessary), and the daily averaged TAO buoy winds were computed. No trends were removed. Note that the period over which it was possible to compute the RMS difference varies from buoy to buoy, so there can be significant change from one buoy to another. The buoys along 110°W, 140°W and 165°E had the longest time series; other buoys had data for as little as a year, because they were recently deployed. The results for a large sampling of the buoys are presented in Figure II.4. Overall, the zonal and meridional wind results were comparable. Maximum RMS differences were about 2.5 ms^{-1} and minimum differences about 1ms^{-1}. The largest values tended to be in the ITCZ and SPCZ regions, although the differences along 165°E were 2 ms^{-1} or more from 5°N to 9°S. The smallest values tended to be in the eastern south-easterly trade winds.

The implication of these values comes following comparison with the magnitude of the WWE signal (which I later shall show is 8 to 20 ms^{-1}) and with the accuracy of the TAO measurement. The wind sensors themselves are claimed to be accurate to about 0.2 ms^{-1}

pre-deployment and are estimated to drift by up to 0.5 ms^{-1} during 1 year of activity (Mangum, Freitag and McPhaden 1994). It should also be noted that the wind measurements on the buoys are done at 4m from the surface, while the ECMWF winds are at 10m. According to a stability correction algorithm developed by W.G. Large (Large and Pond 1981) to adjust wind speed from a height z to a height of 10m., I found that the wind speed correction is typically 10% or less. Thus without height adjustment I may expect errors of about 0.5 ms^{-1} on a wind of 5 ms^{-1} or 1 ms^{-1} for 10ms^{-1} wind. Since I cannot height-adjust the TAO winds because the information required to make the stability correction is typically not available, I suggest a plausible expected mean error on the TAO data to be 0.7 to 1.5 ms^{-1} under typical moderate WWE conditions. Thus the disagreement between the TAO data and the ECMWF data is similar to the uncertainty in the TAO data; and, since WWEs typically have maximum zonal winds in excess of 10ms^{-1}, use of the ECMWF analysis gives us an acceptable signal to noise ratio.

I am unable to determine the accuaracy of the ECMWF high-frequency data outside the region spanned by the TOGA/TAO array. Since the ECMWF incorporates TAO data into its analysis, an agreement with TAO is not surprising. Since the main signals in the analysis are in the regions covered by the TAO array, and the signals are large relative the seasonal variance, I expect the ECMWF analysis to be satisfactory. The ECMWF, because of its grid-spacing and time sampling (2.5° and 12 hours) should be expected to deviate from observed winds expecially in the region of the ITCZ. These differences could be large instantaneously. In the TAO buoys nearest the ITCZ (bouys along 8°N, 180°-140°W), the zonal wind rms difference between ECMWF and TAO is not noticeably different from that in other regions, however the meridional wind rms difference is. Because of this, I am most cautious about subtle results in and near the ITCZ region, especially those relating to variations in meridional winds.

Ideally, the TAO array would be dense enough to permit characterization of the

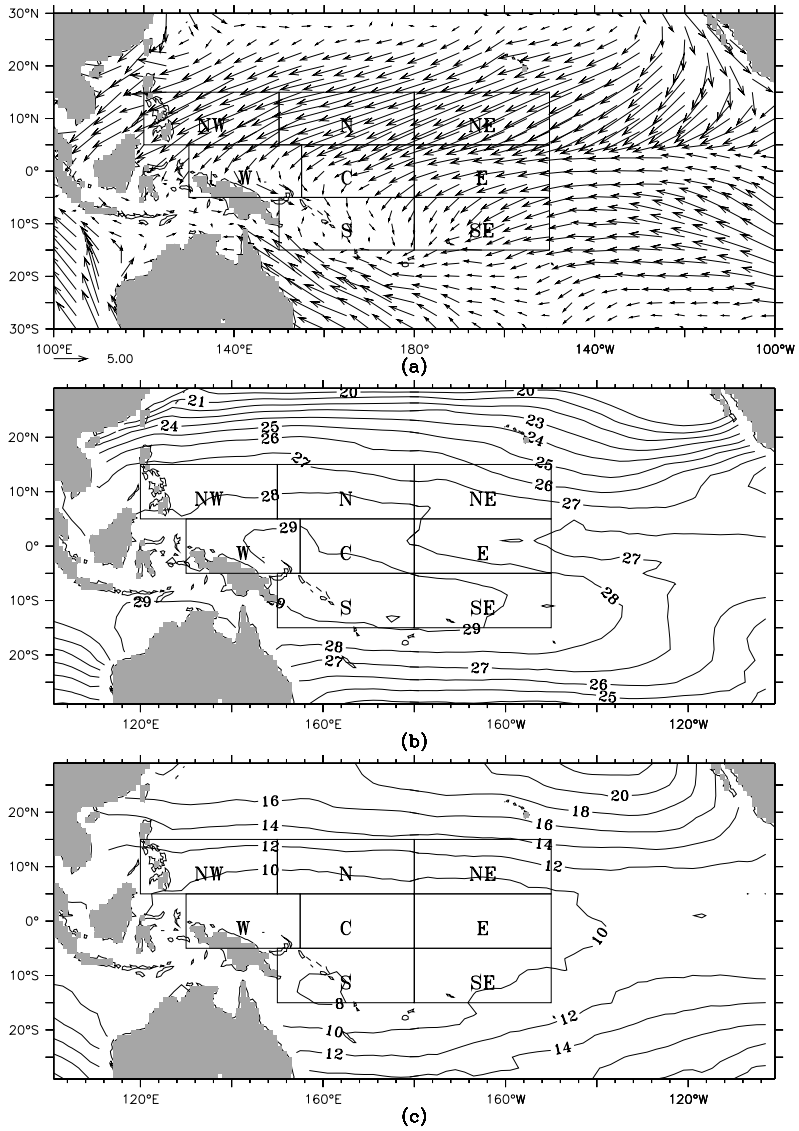

Figure II.5. Classification regions supperimposed on the March (a) ECMWF climatological winds (1986-95), (b) COADS climatological SST, (c) COADS cliamtological SLP-1000. Scale vector is 5ms^{-1} for (a); contour intervals are 1°C for (b) and 2 mbar. for (c).

structure of WWEs itself. However the area coverage and the spatial separation of buoys significantly limit its ability to provide the needed spatial resolution. In its present configuration the TAO array is useful in that it provides data to the wind analyses (and thus should improve their realism) and it provides the information needed to define the likely errors in the analysis. But the ECMWF wind analysis itself is required to carry out the work described below.

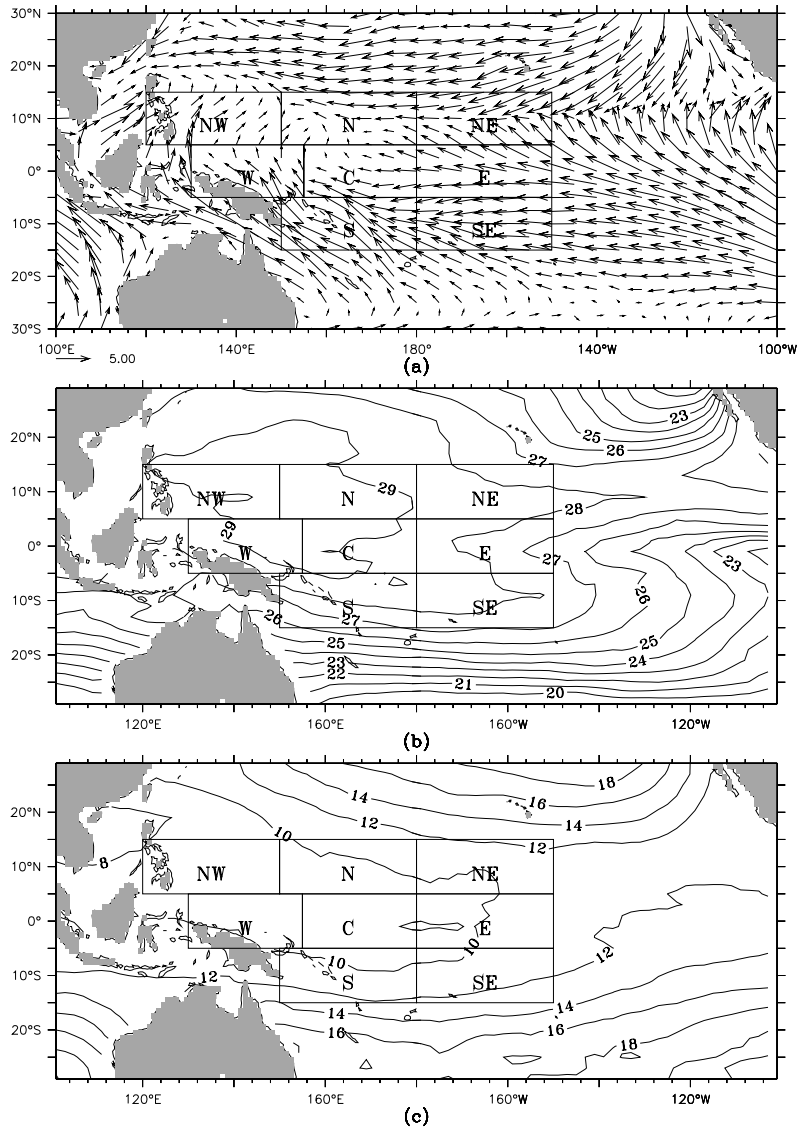

Figure II.6. Same as Figure II.5 except for the month of September.

II.3. Methods

This section describes how the WWEs are classified and how the composite WWEs are computed. First how I came to define the different types of WWEs is described; then the quantitative classification criteria used for each are described. The number of events of different types that follow from the application of these classification criteria to the 1986-1995 ECMWF wind anomaly fields is shown. Finally, the details of the WWE compositing technique are discussed. Description of the analysis to determine the statistical significance of the features of the composites is included in Appendix A.

a. Classification

I began by looking at vector plots of the wind and wind anomalies over the tropical Pacific, for every 12 hour analysis period in the data set. I then highlighted the vectors with westerly anomaly and looked at all the anomaly plots again. I found that westerly wind anomalies of substantial scale tended to occur in particular regions, and not to show major translation during their lifetimes. This suggested that a good classification scheme could be based upon the location of maximum westerly wind anomaly.

Based on the wind anomaly patterns I saw, I defined eight regions to serve as the framework for the classification scheme. These regions, which cover most of the ocean from 120°E to 150°W and 15°S to 15°N, were named according to their location relative to each other. The zonal dimension of these regions is about 30° of longitude, and the meridional dimension is 10° of latitude. Each contains five ECMWF grid-points in the meridional direction, and twelve to thirteen points in the zonal direction. To help place them in the context of the large scale environment of the region, the regions are superimposed upon the COADS climatological (1946-1995) mean winds, SST and SLP for March (Figure II.5) and for September (Figure II.6). Note that there are substantial changes in the environment in each region between March and September.

In order to systematically identify and analyze WWEs, it is useful to introduced a quantitative definition for their existence, within the context of the classification scheme. A WWE of type ***X*** is defined as any period of three or more days for which the 10-m zonal wind anomaly, averaged over region ***X*** and smoothed by a three point triangle filter in time (half-power point at 2.75 days), exceeded 2 ms^{-1}. To label and organize the events, an event's center day was defined to be the day for which the zonal wind anomaly, averaged over the region, was greatest. With these classification criteria all the westerly wind events identified, by region (type) and center date.

It is useful to describe the intensity of the WWEs according to their "duration",

"maximum averaged anomaly", "maximum point anomaly" and "wind measure". The duration of each WWE is defined to be the time span between when the identification criteria are first met and when the identification criteria are no longer satisfied. The maximum averaged anomaly is defined to be the zonal wind anomaly averaged over the classifying region on the center day of the event. The maximum point anomaly is the maximum zonal wind anomaly within the classifying region, on the center date. The wind measure is defined as the time integral of the zonal wind anomaly, averaged within the classifying region and smoothed by a three point triangle filter in time (half-power point at 2.75 days), over the event duration.

Not every period of westerly wind anomalies fit perfectly into the classification scheme. In particular, sometimes substantial westerly wind anomalies occurred in adjacent regions at the same time. This led to an additional sub-classification of WWEs into overlapping and non-overlapping events. Overlapping events were defined to be events which were identified in two regions which shared more than half an edge and whose center dates were within three days of each other. For each pair of overlapping events, the maximum averaged anomaly for each event was compared, and the event was classified as an event of the type for which the maximum averaged anomaly was greatest. There were then two lists of dates, one with all the events, which shall be referred to as the "complete event list", and another with all the non-overlapping events plus the overlapping events classified according to the secondary classification scheme, which shall be referred to as the "non-overlapping event list". Table II.1 summarizes the number of events identified for each type of event in each list.

Table II.1: Number of WWEs identified duirng 1986-95, in each of the classifying regions, for the complete event list and for the non-overlapping event list. (see Section 3.a)

List	NW	N	NE	W	C	E	S	SE
Complete event list	58	28	36	35	62	42	39	51
Non-overlapping event list	51	25	28	28	49	34	29	43

b. Compositing

The basis of the compositing is the identification of the center day (day (0)) for each event of a type "X". The day(0) field for the composite type "X" event is computed by averaging together the wind or wind anomaly field for all the type "X" event days(0). Composite day(±n) is computed similarly from each of the days(±n) for type "X" events. The composites are evaluated for day(-9) through day(9) for each of the eight types of WWEs, resulting in a 20 day composite event. The composites are evaluated using all the events from each type of WWE.

For each type of event, then, the composite is evaluated according to:

Where **U** is the composite vector wind anomaly, **u** is the instantaneous vector wind anomaly, x is the zonal location, y is the meridional location, $\{\tau_i\}$ are the center days for the individual events, t_n [-9,10] is the event day, and N is the number of events to be composited. To study the effect of event overlap in the averaging process, two sets of composite westerly wind events were generated: one using the dates in the complete event list, the other using the dates in the non-overlapping event list. The two composites were not different in any significant qualitative aspect, so I present only the composites generated from the complete event list. The composite wind fields for each type of event were similarly computed.

II.4. Composite results

In this section I present the results of the composite analysis. I show vector wind anomaly maps for selected days of each type of event. I also present vector maps of the wind field on the center day (day(0)) for each type of event. I shall show that a simple model structure provides a convenient way to define the zonal, meridional and temporal scales of

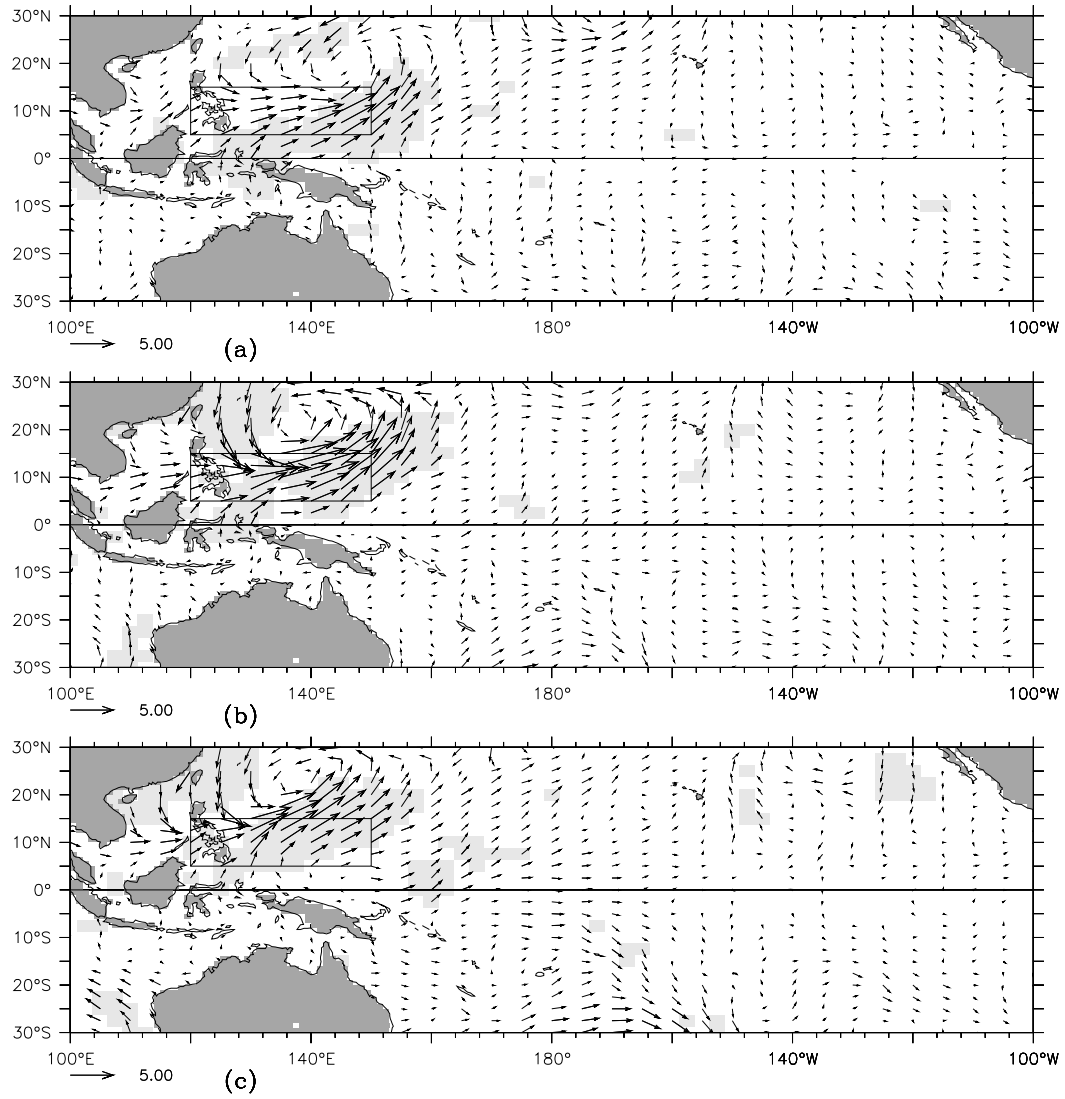

Figure I.I.7. Type NW composite wind anomalies for (a) Day (-2), (b) center day, and (c) Day (2). Classifying region is indicated by thin lined box. Bold vectors (shading) indicate the zonal (meridional) component is significant at the 95% level. Scale vector is 5 ms^{-1}.

the zonal wind anomalies for each of the composites and I present the scales of each event from this perspective.

a. Vector maps

Daily wind anomaly vector maps for days (-9) through (+9) for each of the eight types of WWEs were generated, the full set of maps is shown in Vecchi and Harrison (1997). Here I present only selected maps to illustrate the patterns when the wind anomalies are substantial. For each type of event I show the wind anomaly on day(-2), day(0) and day(+2)

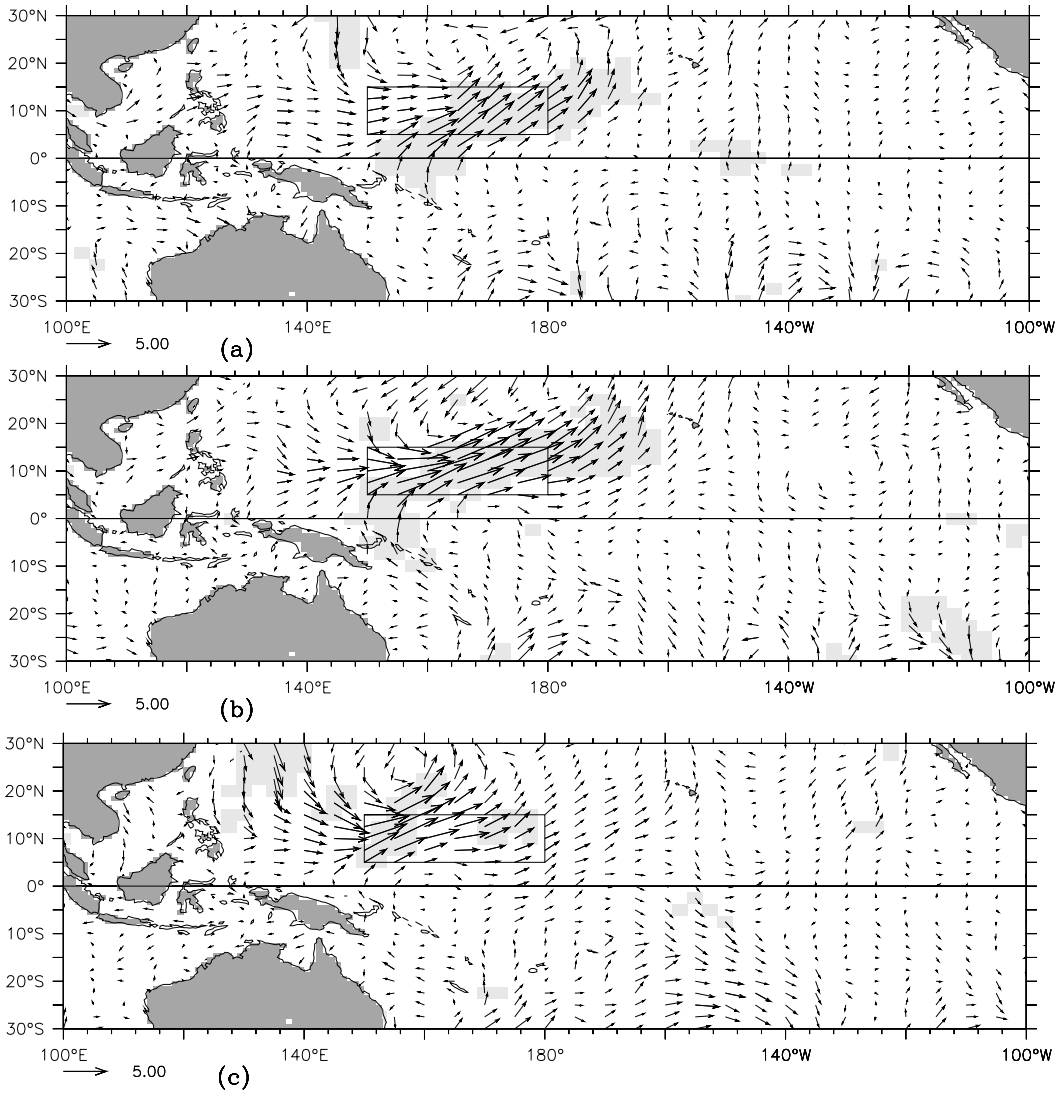

Figure II.8. Same as Figure II.7, except for type N composite.

(Figures II.7 through II.14). Note in these figures that the region used to define the featured type of event is outlined. The anomalies highlighted as bold vectors have zonal component significant at the 99% level, and those highlighted by a shaded background have meridional wind component comparably significant. Statistical significance was determined by a Student's-*t* test (Appendix A).

I describe qualitatively the features of the patterns that merit note, and follow the atmospheric convention that an easterly wind is a wind from the east, etc. It is helpful to introduce composite wind magnitude labels as follows: weak (u£2 ms^{-1}), moderate (2ms^{-}

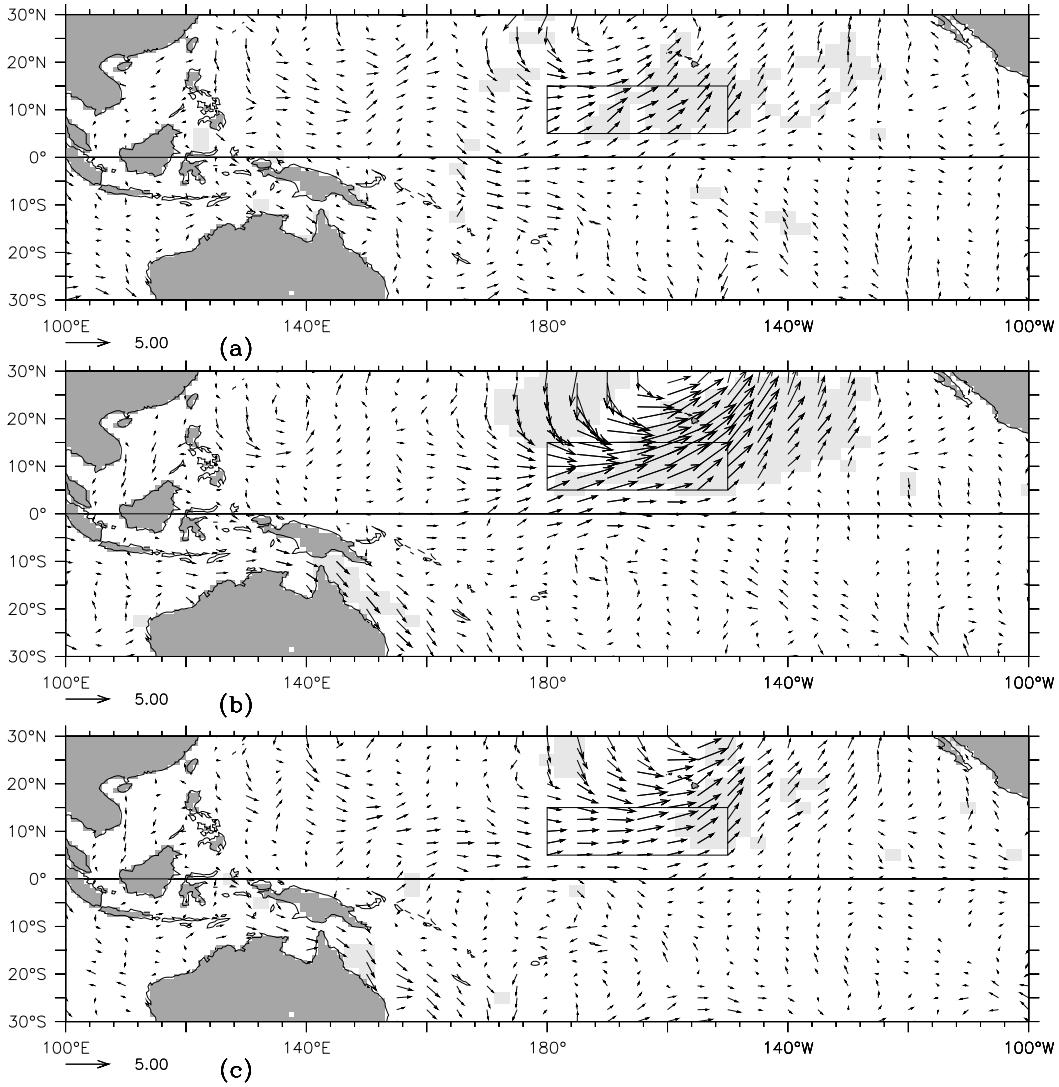

Figure II.9. Same as FigureI I.7, except for type NE composite.

^{1}<u£ 4 ms^{-1}) and strong (u>4 ms^{-1}). It is simplest to identify common elements in the Composite events by sorting them into Northern Regions (NW, N and NE); the Equatorial Regions (W, C and E); and the Southern Regions (S and SE).

i) NORTHERN REGIONS: NW, N AND NE (Figures II.7, .8 and .9):

Each of these events has strong meridional and zonal wind anomalies. Although the areas of maximum significance are principally occupied by moderate to strong westerly and south-westerly anomalies, there are clear suggestions that these events are associated with anomalously cyclonic circulations, with moderate to strong easterlies and northerlies

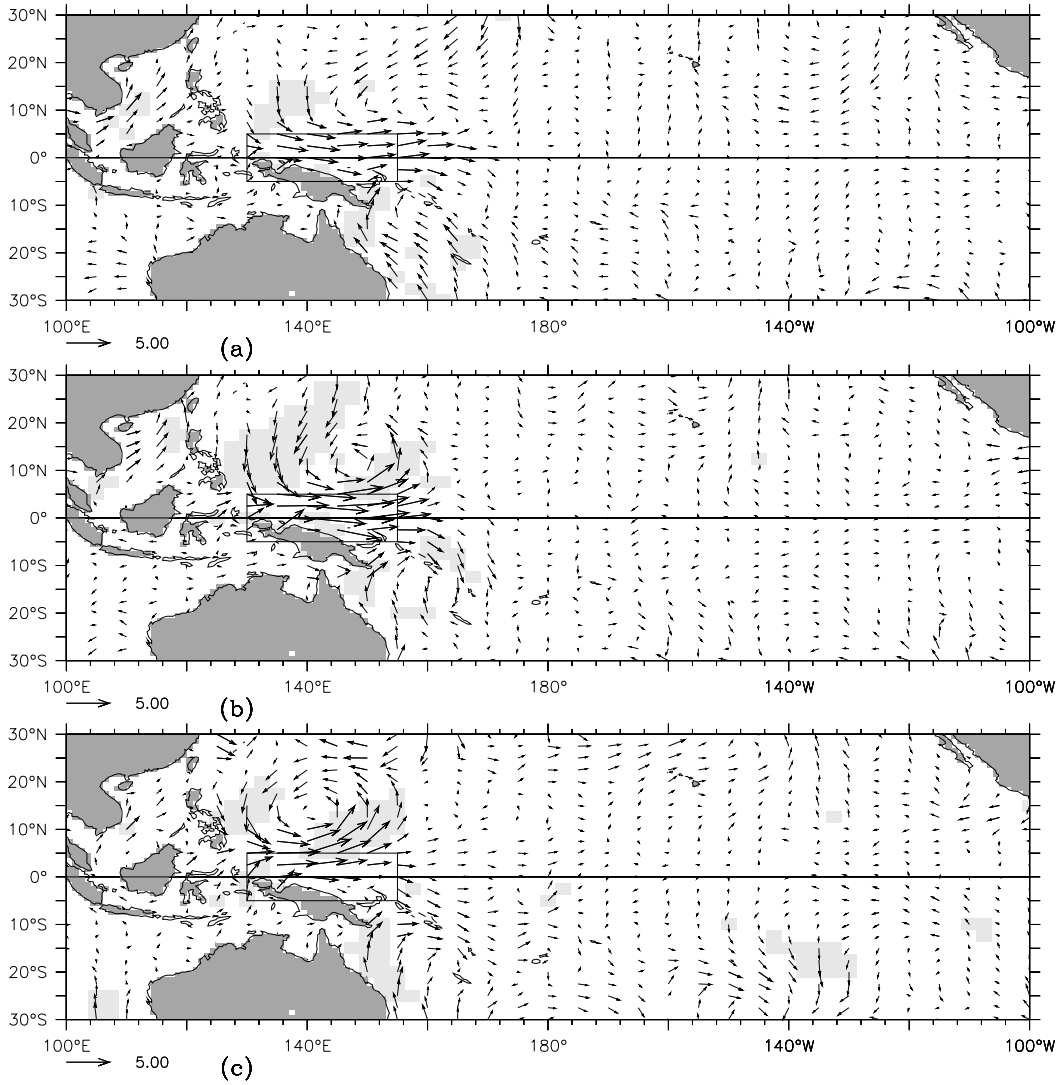

Figure II.10. Same as Figure II.7, except for type W composite.

to the north and west of the regions. All of these events also show a modest translation of the area of maximum anomalies during the event. The type N and NW events show north-westward displacement throughout the event, while the type NE event shows an eastward displacement throughout the event.

The NW and N type events share additional common features. Both types of events have periods of distinct weak to moderate cross-equatorial inflow from day(-3) until day(2) for the type NW event, and from day(-3) until day(0) for the type N event. There is also well defined inflow from west of the cyclonic feature from day(-2) to day(3) for the type NW

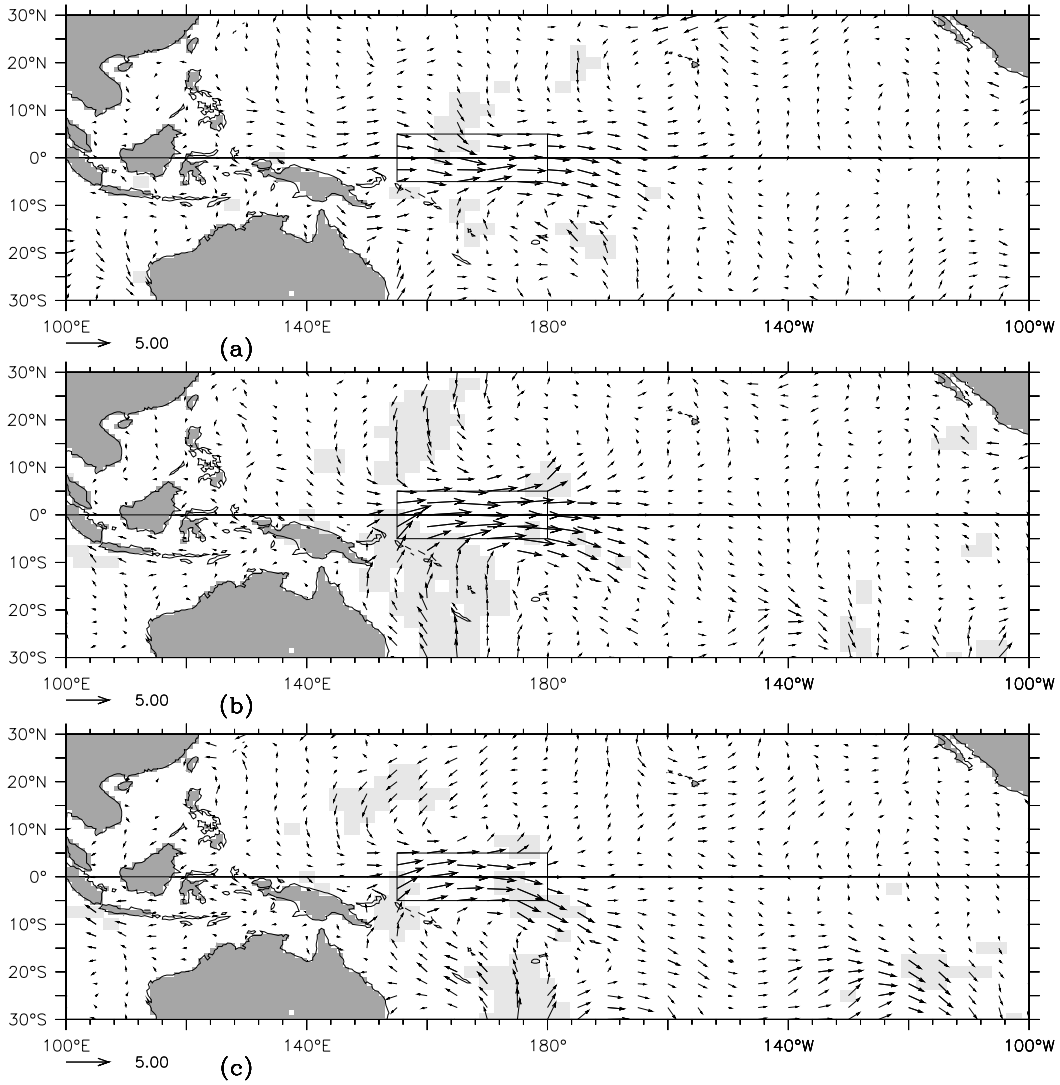

Figure II.11. Same as Figure II.7, except for type C composite.

event, and from day(-2) to day(2) for the type N event. The circulation is more complicated than a simple cyclonic flow.

The NW and NE type events share periods of weak to moderate equatorial westerly anomalies. For the NW type events, there is a period of equatorial westerlies to the south of the classifying region prior to the center day, lasting eight days, centered around day(-5), when the maximum equatorial westerlies occur; there are also weak equatorial westerlies from day (2) through day(5), to the southeast of the region. For the type NE events, equatorial westerlies to the south of the classifying region occur during the period of maximum

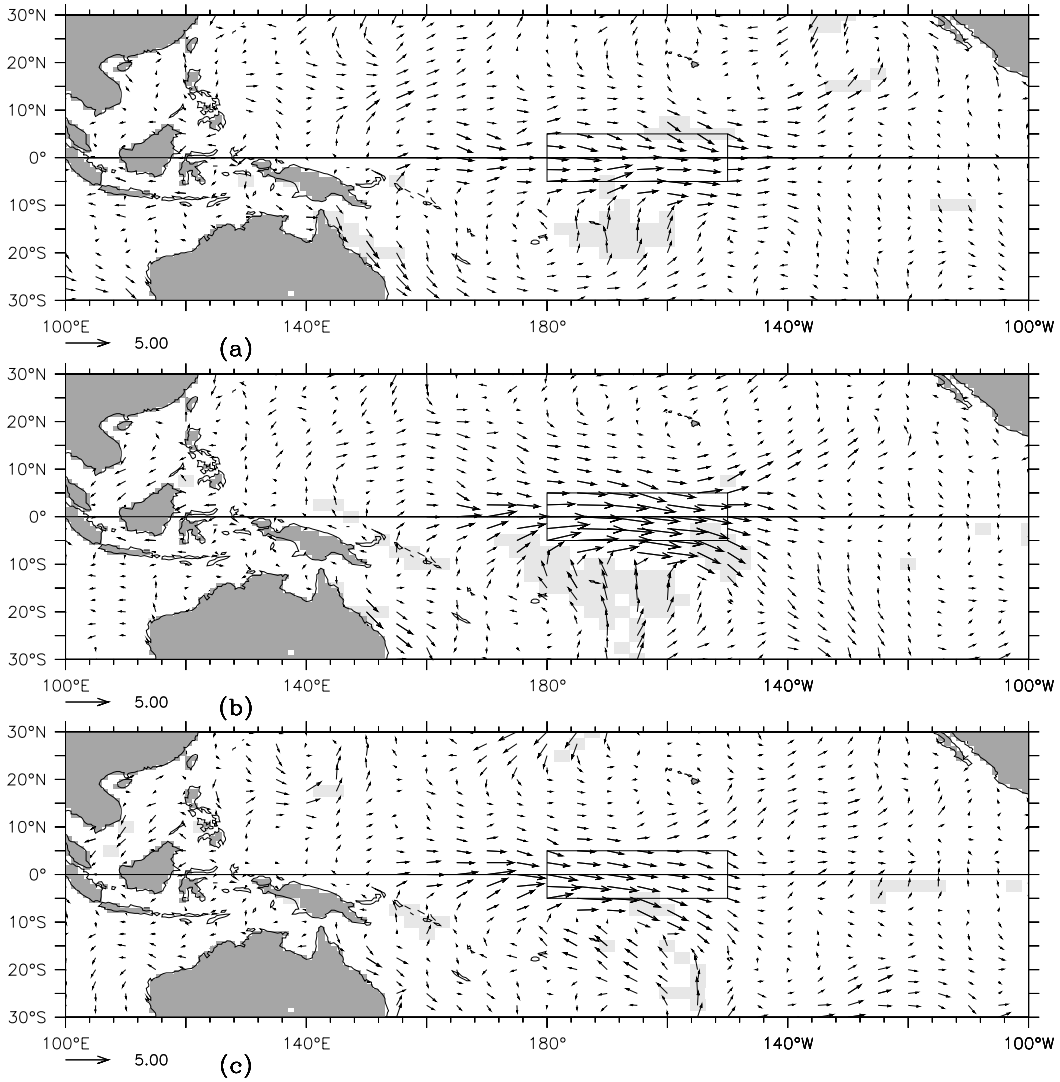

Figure II.12. Same as Figure II.7, except for type E composite.

anomaly in the region, last for three days and have their peak amplitude on the center day of the event.

ii) EQUATORIAL REGIONS: W, C AND E (Figures I10, .11 and .12):

For each of the equatorial WWEs the maximum anomalies are primarily zonal, with periods of moderate meridional inflow to the western part of the regions. The equatorial westerlies in all three events are meridionally contained within the defining region, but their zonal extent can be substantially larger than the defining region. The meridional inflow typically can be found at least 20 degrees away from the equator, but can extend as far

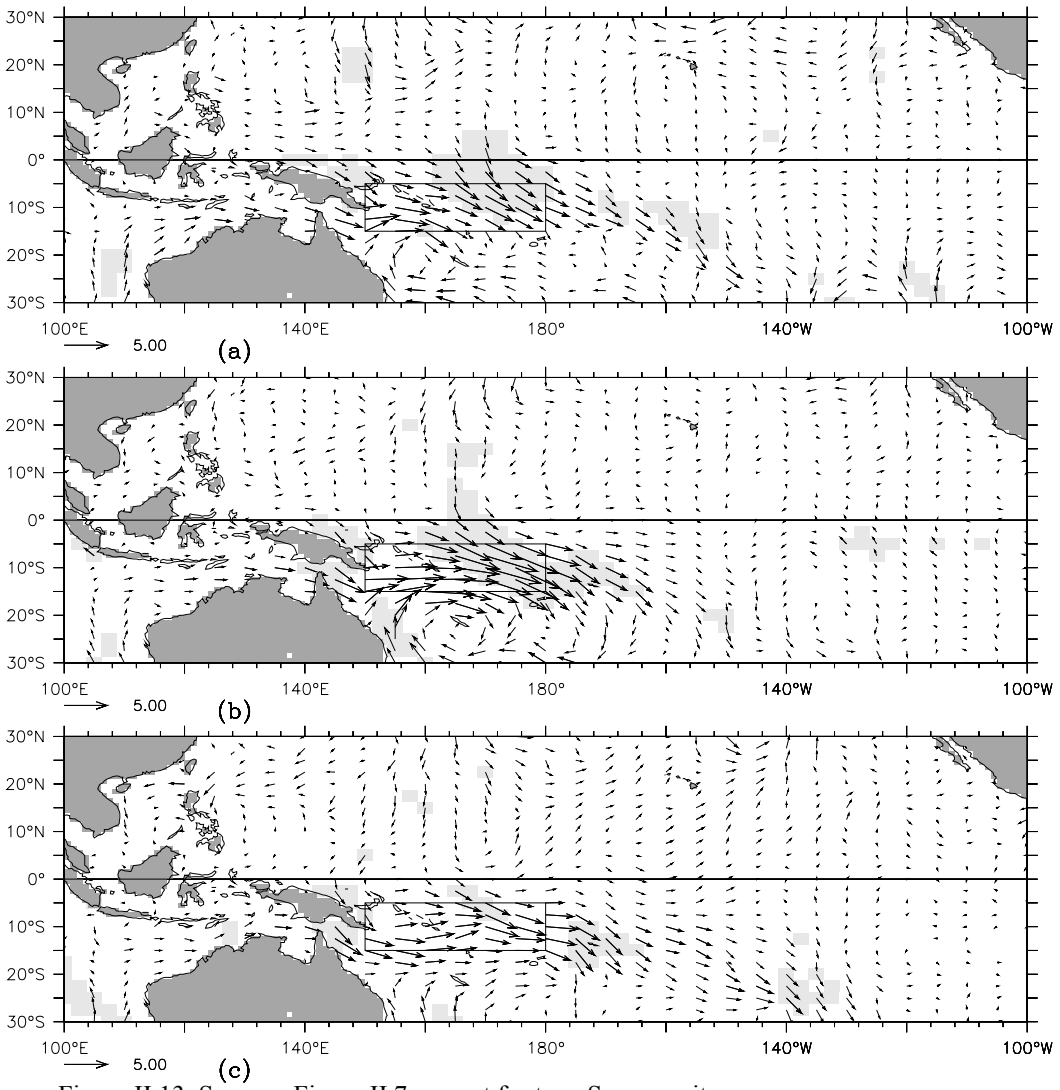

Figure II.13. Same as Figure II.7, except for type S composite.

as 30 degrees (the southerly inflow on day(0) of the type C event). For the type C composite event, the zonal wind anomalies are close to symmetric with respect to the Equator, while for the types W and E event there is a pronounced asymmetry. The type W composite event has symmetric anomalies in the early part of its evolution, while as day(0) is approached the anomalies become more pronounced to the north of the Equator. The type E composite event has its largest anomalies to the south of the Equator.

For the type W event there is moderate southerly inflow during event days(-5) and (-4) (Vecchi and Harrison 1997), followed by a moderate northerly inflow that begins on the

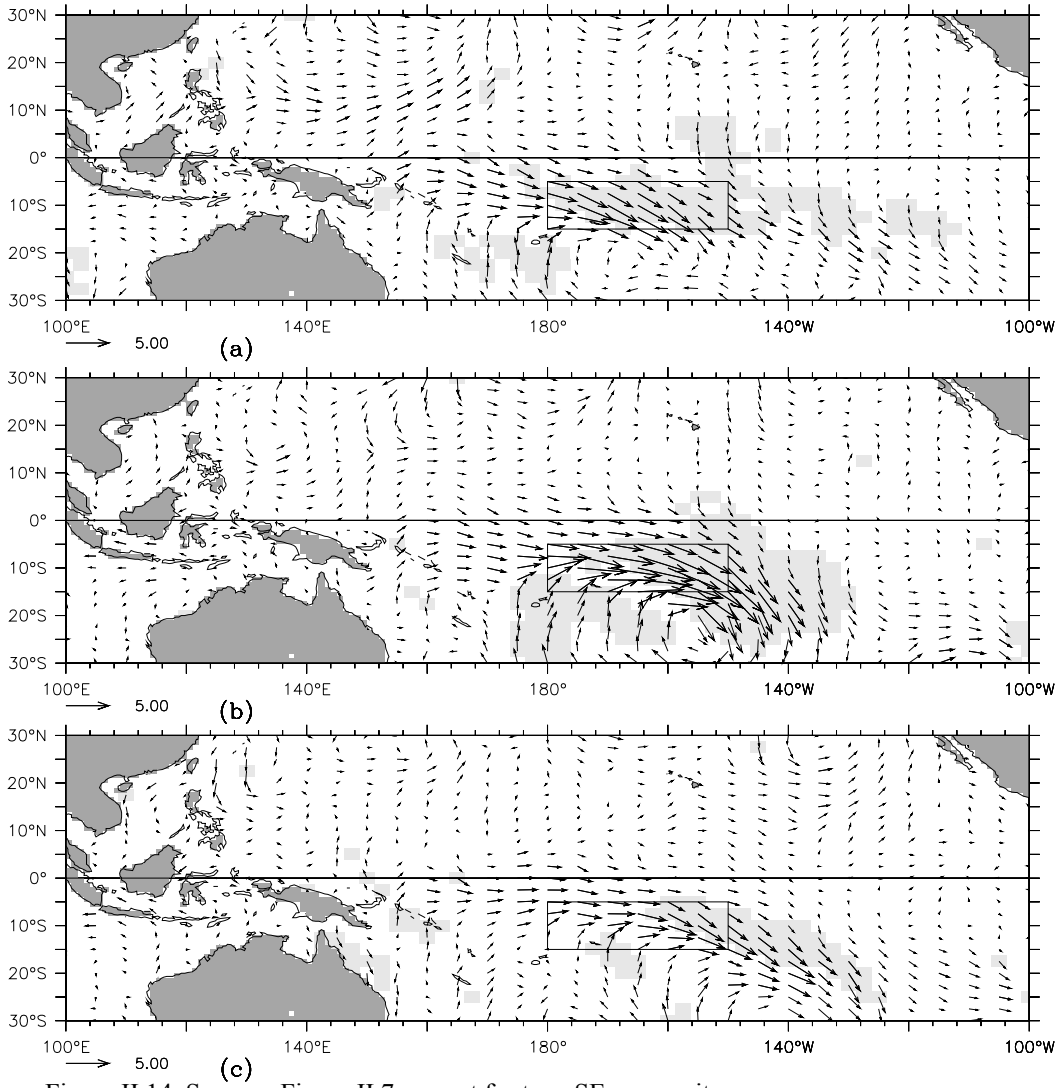

Figure II.14. Same as Figure II.7, except for type SE composite.

center day and an anomalous cyclonic circulation subsequently develops. For the type C event there is moderate northerly and southerly inflow beginning on day(-1) and ending after day(1). For the type E event, there is moderate southerly inflow beginning on day(-2) that continues until the center day. Both the type W and the type E events exhibit a translation of the area of maximum anomaly. The W type event has a translation towards the northwest after the center day. The type E event has a westward translation after the center day.

iii) SOUTHERN REGIONS: S AND SE (Figures II.13 and .14):

Both of these composite events have a moderate to strong meridional component as well as strong westerly anomalies near day(0). Although most of the significant anomalies are westerly and northwesterly, there are also moderate to strong easterly and southerly anomalies suggesting a pattern of anomalously cyclonic flow. The events also exhibit eastward translation of the area of maximum anomaly throughout the event.

Both of the composite events exhibit moderate cross-equatorial inflow on and immediately preceding the center day. The cross-equatorial inflow for the type S event occurs through the northwestern corner of the region as well as the eastern half of the northern edge of the region, from day(-2) through day(0). For the type SE event, the cross-equatorial flow is most persistent north of the eastern corner of the region, from day(-2) through day(0). Both events exhibit strong inflow from the west on the days before and during the period of maximum anomaly. The westerly inflow for the type S event, begins on day (-9) and extends as far west as the Indian Ocean. So the structure of the circulation of these events, like that of the type N and NW events, is not just a simple cyclonic one.

The type SE event has persistent weak to moderate equatorial westerly anomalies on the days surrounding the center day. The equatorial westerlies are stronger to the south of the equator than to the north of it. The type SE event also has moderate southerly inflow from higher latitudes on the days preceding and on the center day.

b. Center day wind maps

Figures II.15 through II.17 show vector plots of the center day of the total wind composite, for each type of WWE. As before, it is helpful to discuss the composites by grouping the events by northern, equatorial and southern regions. I shall refer to many of the features described in the previous section; see Figures II.7 through II.14 as needed.

i) NORTHERN REGIONS: NW, N AND NE (Figure II.15):

The anomalously cyclonic circulations in the type NW and N anomaly composites manifest themselves as cyclonic wind patterns in the wind composites. The type N wind

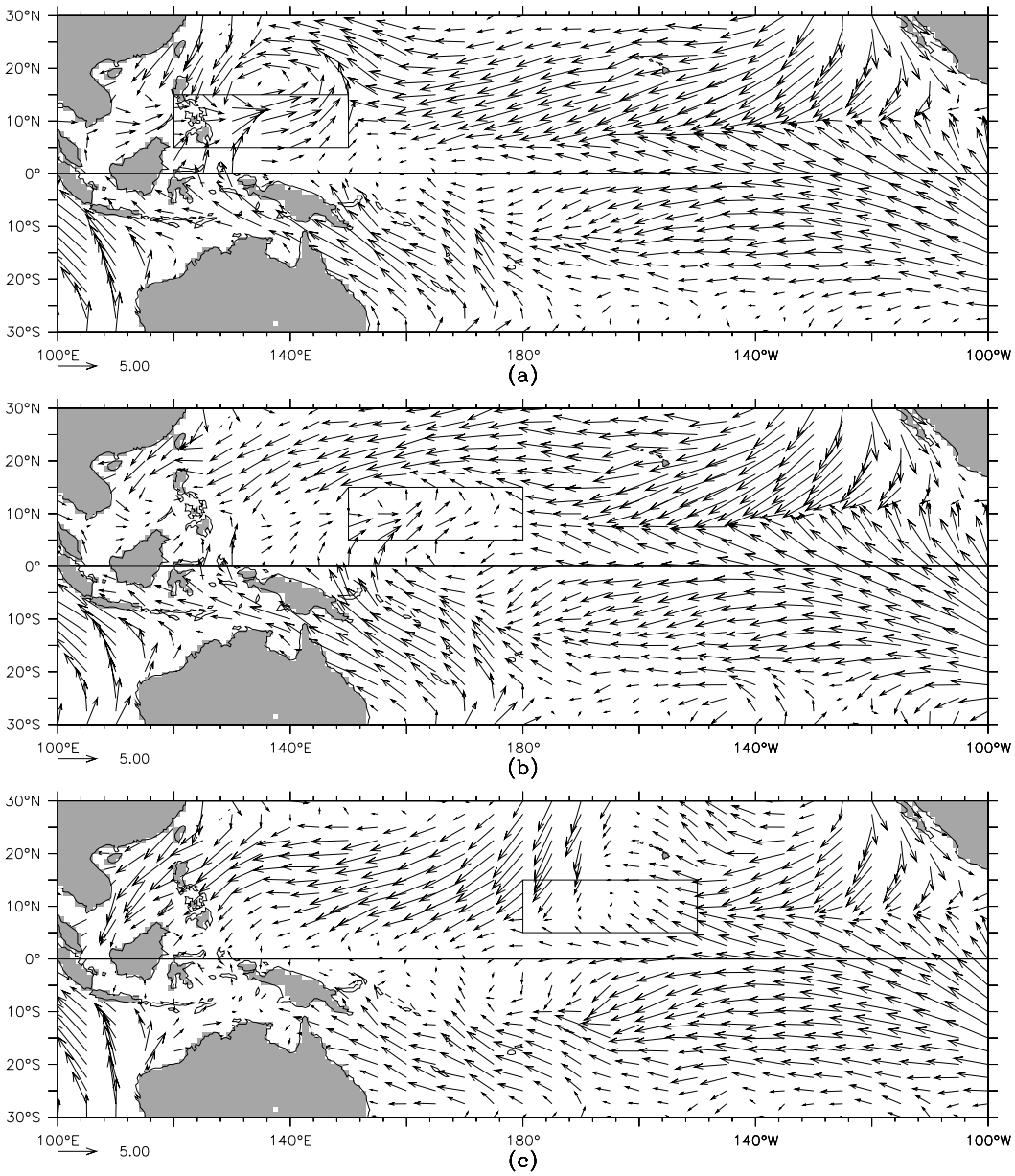

Figure II.15. (a) Type NW, (b) type N, and (c) type NE composite WWE 10-m wind vector map, for event center day. Scale vector is 5 ms^{-1}. Classifying region is indicated by the box.

pattern indicates a reversal of the north-easterly trades within the classifying region. The situation differs for the type NE event, for which the wind composite indicates a trade wind break, but not a cyclonic wind pattern, because of the strength of the north-easterly trades in that region. The translation of the area of maximum anomaly noted in the anomaly plots, is also apparent in the full sequence of wind composite figures (Vecchi and Harrison 1997).

The cross-equatorial inflow noted in the type NW and N event anomalies is also

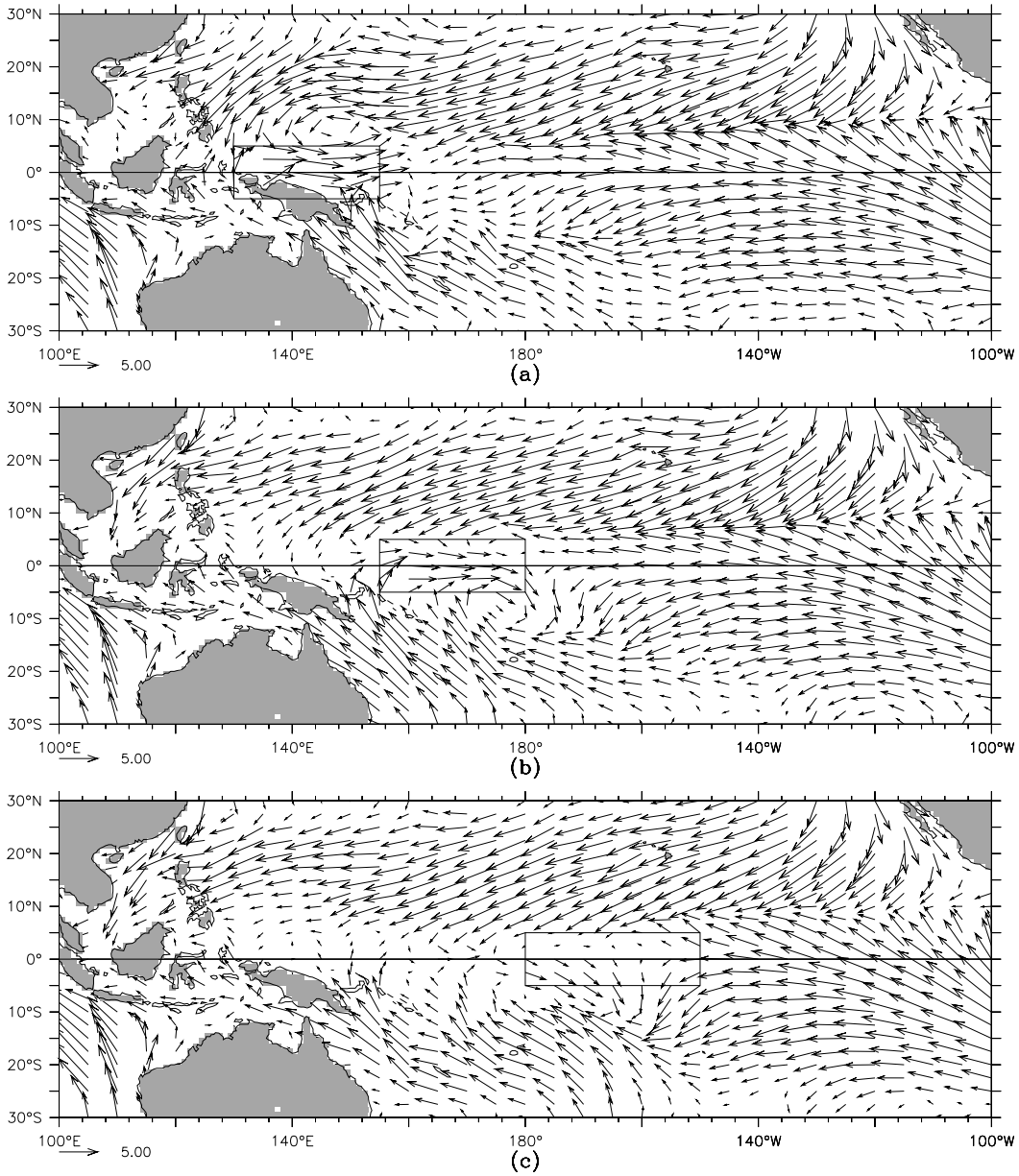

Figure II.16. (a) Type W, (b) type C, and (c) type E composite WWE 10-m wind vector map, for event center day. Scale vector is 5 ms^{-1}. Classifying region is indicated by the box.

apparent in the wind composites, but the anomaly inflow from the west is not clear in the winds themselves. The equatorial westerly anomalies in the type NW event appear as actual equatorial westerly winds to the south of the region. The equatorial westerly anomalies noted in the type NE events do not appear as equatorial westerly winds here.

ii) EQUATORIAL REGIONS: W, C, AND E (Figure II.16):

For the type W and C events, the primarily zonal westerly anomalies in the region

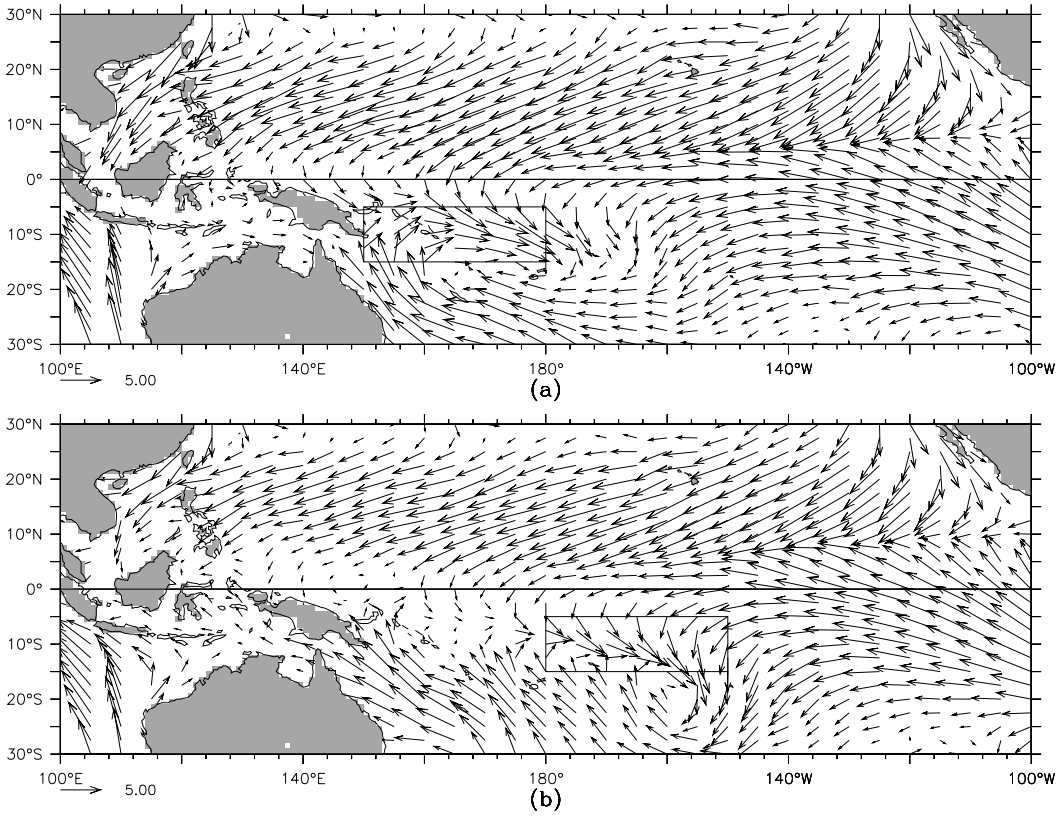

Figure II.17. (a) Type S, and (b) type SE composite WWE 10-m wind vector map, for event center day. Scale vector is 5 ms^{-1}. Classifying region is indicated by the box.

appear as primarily zonal westerly winds. However, for the type E event, the wind field has a noticeable meridional component. Also, while the anomalies for the type C event were centered about the equator, the winds are asymmetrical with the greatest westerly amplitudes south of the equator (this is due to the seasonality of the strong type C events (Section 6.a), which tend to occur in austral winter when the climatological winds south of the equator are westerly). The equatorial asymmetry of the type E zonal wind anomalies is also noticeable in the wind composite.

The southerly inflow anomaly in the type W and C events appears as a strengthening of the already prominent south-easterly trade winds to the east of Australia. For the type E event, southerly inflow in apparent, and is linked to a cyclonic circulation pattern to the south-west of the region, which translates westward. For the type W event the northerly inflow anomaly is discernible in the winds, so is the cyclonic anomaly circulation which

tends to move north-westward. For the type C event the northerly inflow anomaly is overwhelmed by the strong trade winds, but a cyclonic wind circulation forms, centered to the south of the region, which does not propagate from day (-4) when it first appears to day (4) when it dissipates.

iii) SOUTHERN REGIONS: SE AND S (Figure II.17):

Both of these composite events display strong meridional winds, as well as zonal winds in the classifying regions. The type SE composite winds shows a reversal of the south-easterly trades. The winds also have a cyclonic pattern to them, which translates to the east as it decays for the type S events, and decays quickly for the type SE event. The cross equatorial inflow anomaly for the type S event produces cross-equatorial flow in the winds. For the type SE event, there is no cross-equatorial flow in the area of cross-equatorial anomalies. For the SE type event the anomalously southerly inflow enhances the south-easterly trade winds to the west of the trade wind reversal.

c. Scales

Now I turn to the problem of defining the scales of the composite WWEs. Table II.2 shows the duration, maximum averaged anomaly, wind measure and maximum point anomaly for each of the composite WWEs (Section II.3.a). The events have a duration in the range of 4.5-5.5 days, except the type NE event (4 days). The maximum averaged anomaly is in the

Table II.2. Duration, maximum averaged anomaly, wind measure and maximum point anomaly for each composite WWE. Quantities as defined in Section 3.a.

Region	Duration (days)	Maximum averaged anomaly (ms^{-1})	Wind measure (10^6 m)	Maximum point anomaly (ms^{-1})
NW	5	4.0	1.3	7.2
N	5.5	4.6	1.6	6.6
NE	4	4.2	1.1	6.3
W	4.5	3.9	1.1	6.9
C	5.5	4.4	1.4	6.4
E	4.5	4.1	1.2	5.5
S	5	4.4	1.4	6.4
SE	5	4.7	1.4	6.7

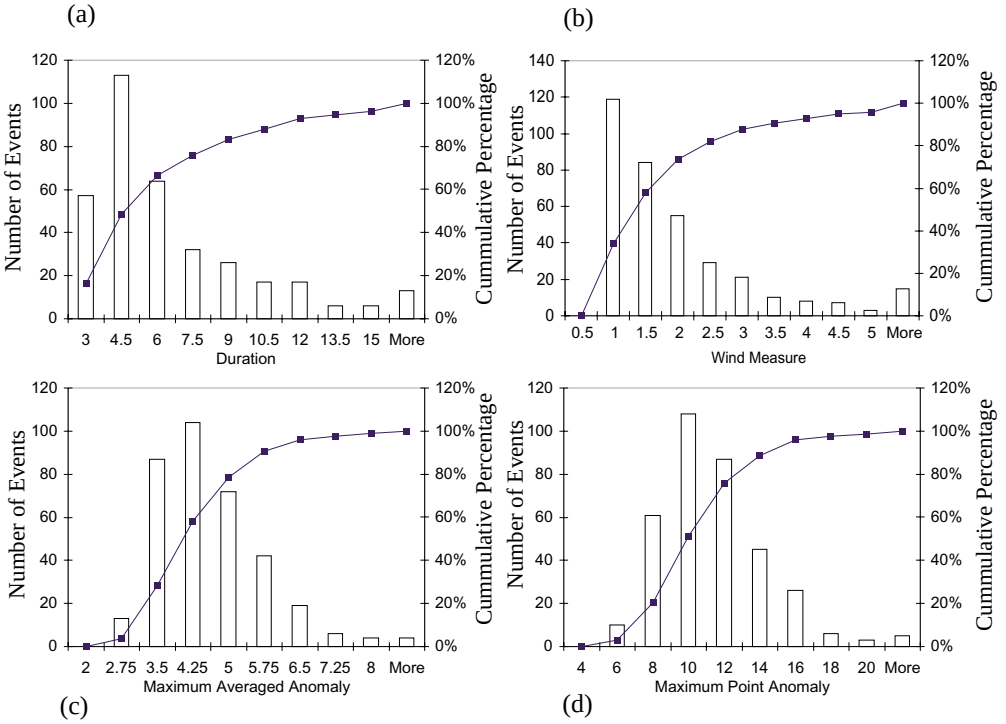

Figure II.18. Histograms of WWE (a) duration, (b) wind measure, (c) maximum averaged anomaly, and (d) maximum point anomaly, for WWEs of all types occuring during the 1986-1995 period. Bar graph indicates the number of WWEs occurring within the labeled bins, and the line graph indicates the cumulative percentage of events at each bin. Units are days for duration, 10^6 m for wind measure, and ms^{-1} for maximum point anomaly and maximum averaged anomaly. Quantities as defined in Section 3.a.

range of 3.9 to 4.7 ms^{-1}; the strongest events are type SE (4.7 ms^{-1}) and type N (4.6 ms^{-1}), and the weakest is type W (3.9 ms^{-1}). The wind measure for all the events is between 1.1 and 1.6 x 10^6 m; the strongest event is type N (1.6 x 10^6 m). The events have maximum point anomaly between 6.3-7.2 ms^{-1}, except the type E event (5.5 ms^{-1}).

Histograms for duration, maximum point anomaly, maximum averaged anomaly and wind measure for all the events over the entire record are shown in Figure II.18. The frequency distributions for the individual events are similar to those for the entire record, so I do not present distributions for each type of event; see Vecchi and Harrison (1997) for breakdown by event type. From Figure II.18 it can be seen that approximately 50% of the WWEs in the record have a duration greater than 3 and less than 6 days (recall the composite WWE durations vary between 4 and 5.5 days). For maximum averaged anomaly, ap-

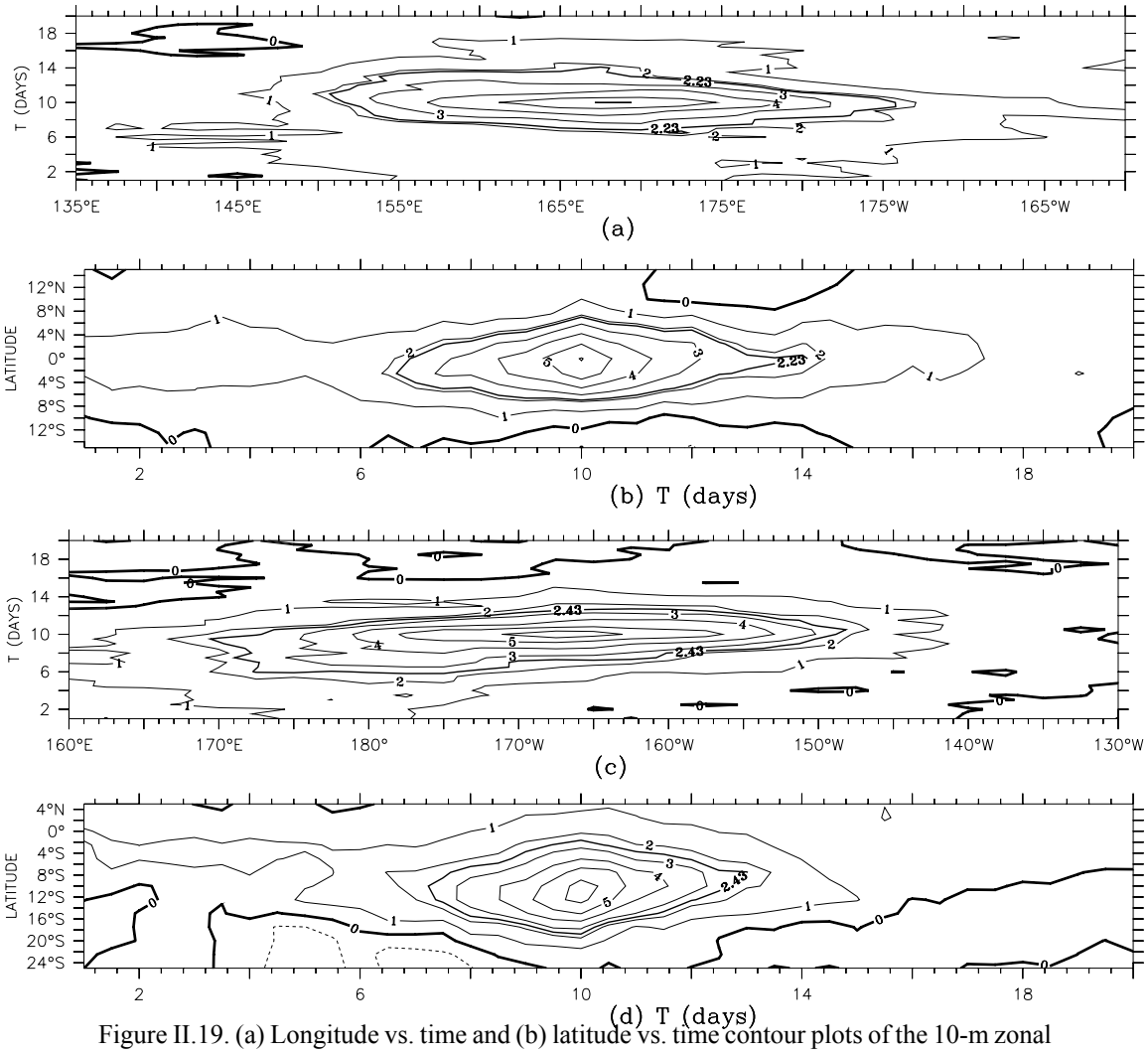

Figure II.19. (a) Longitude vs. time and (b) latitude vs. time contour plots of the 10-m zonal wind anomaly for the type C composite WWE; and (c) longitude vs. time and (d) latitude vs. time contour plots for the type SE composite WWE. Contour intervals are 1 ms^{-1} and the dark contour indicates the e^{-1} level of the zonal wind anomaly. Center day of the event is day 10 on the time axis.

proximately 50% of the events have values greater than 3.5 ms^{-1} and less than 5 ms^{-1}, and the composite WWE values are between 3.9 and 4.7 ms^{-1}. For wind measure, approximately 40% of the events have wind measure between 1 x 10^6 m and 2 x 10^6 m (composite WWE wind measures vary between 1.1 and 1.6 x 10^6 m). Since the previous three quantities are large space scale linearly averaged quantities, they are not affected a great deal by the smoothing effects of compositing. For the maximum point anomaly the smoothing effects of the averaging process are evident. The maximum point anomaly of the composite events

varies between 5.5 and 7.2 ms^{-1}, but fewer than 20% of the WWEs had maximum point anomaly values which are that low; this is because much of the small scale structure of the individual events has been smoothed out by the averaging.

To characterize the behavior of the zonal wind anomaly field as simply as possible, I formulated a simple analytical model for it. I constructed x-t and y-t contour plots of the zonal wind anomaly for each type of event (see Vecchi and Harrison (1997) for the full set of these plots), and found the zonal wind anomaly to be sharply bounded in space and time. Examples of Type C and SE composite suffice to illustrate the typical situation (Figure II.19).

$$U(x,y,t) = U_o \exp\left[-\left(\frac{x - X_o - c_x t}{L_x}\right)^2\right] \times \exp\left[-\left(\frac{y - Y_o - c_y t}{L_y}\right)^2\right] \times \exp\left[-\left(\frac{t}{T}\right)^2\right]$$

A Gaussian in (x,y,t) with translating center to is used define the scales of the events: Where U is the model zonal wind anomaly field, U_o is the maximum point anomaly, (X_o, Y_o) is the geographic center, (c_x, c_y) is the translational velocity, (L_x, L_y) are the spatial *e*-folding scales, T is the temporal *e*-folding scale, and x,y and t_n are as in Section II.3.b. The scales for the Gaussian model were computed as follows. The geographic center of the event is identified as the location of the maximum zonal wind anomaly on the center day. The spatial *e*-folding scales were calculated as half the distance between the two closest *e*-folding points

TableII. 3. Table of scales for the composite WWEs according to the simple Gaussian model described in section 4.b.

Region	U_o (ms^{-1})	X_o	Y_o	L_x (10^6m)	L_y (10^6m)	T (days)	c_x (ms^{-1})	c_y (ms^{-1})
NW	7.2	132.5°E	12.5°N	1.4	0.6	3.5	-3.8	2.6
N	6.6	185°E	10°N	2.5	0.7	3	-5.1	0.3
NE	6.3	165*W	12.5°N	1.6	1.1	2.5	1.3	
W	6.9	142.5°E	0°	1.7	0.4	3.5	-1.3	1.3
C	6.4	170°E	0°	1.8	0.6	3		
E	5.5	172.5°E	2.5°S	1.9	0.7	3	-1.3	
S	6.4	170°E	10°S	2.2	0.7	2.5	2.5	
SE	6.7	167.5°W	10°S	1.6	0.7	3.5	3.8	

on either side of the center, along the axis in the direction of interest. Since the center of the event generally moves in time through the region, the instantaneous center of the event is defined as the point with the largest zonal wind anomaly within 50° in the zonal and 30□° degrees in the meridional direction from the geographic center. The temporal *e*-folding scale was half the time between the two closest *e*-folding points on either side of the center day. Using the instantaneous centers as 'path' data, the translational velocity is the mean velocity with which the instantaneous center moved, during the time when the zonal wind anomalies at the instantaneous centers were above the *e*-folding level.

The characteristics of the events are summarized in Table II.3, presented are the maximum point anomaly, geographic center on day(0), spatial and temporal *e*-folding scales, and translational velocities, for each composite WWE. Using the parameters in the table, the maximum point anomaly (U_o) is between 6 and 7 ms^{-1} and the time scale (T) is close to 3 days for each type of event. All but two types of events have meridional length scale (L_Y) of about 700 km (NE has $L_Y \sim$ 1,100 km and W has $L_Y \sim$ 400 km) and zonal length scale (L_X) between 1,400 and 1,900 km (NW has $L_X \sim$ 2,500 km and S has $L_X \sim$2,200 km). Note that the atmospheric baroclinic Rossby radius of deformation varies from (assuming a wave speed of 20-80 ms^{-1}) 650 to 1300 km (Gill 1982), which is in general agreement with the meridional length scales summarized in the table. All but one type of event (C) has zonal translation of its center (values ranging from -5.1 for N and 3.8 for SE); only type NW, N and W events have meridional translation (northward in each case). For the type of events which appear clearly associated with northern hemisphere cyclonic circulation patterns (NW, N and W) the translational direction is consistent with the direction expected of a northern hemisphere tropical cyclone. (Lau and Lau 1992; Joint Typhoon Warning Center 1994a,b; Tsutsui and Kasahara 1996, see Figure IV.4.a)

II.5. WWEs and the TOGA-COARE intensive observations period

So far I have concentrated on describing the composite WWEs (Section II.4.a,b) and have proposed a simple descriptive model for them (Section II.4.c). A natural subsequent question is the extent to which the composite WWEs usefully describe the wind field when particular WWEs are taking place. The TOGA-COARE Intensive Observations Period (IOP) (Webster and Lukas 1992; Lukas *et al*. 1995) offers an example period (November 1992 - February 1993) when WWEs were the focus of a major oceanographic and meteorological field program. The IOP occurred at the end of the warm phase of ENSO, ISOs passed over the western pacific during the program (Chen and Houze 1996; Lin and Johnson 1996), and there were some tropical cyclones as well (McBride *et al* 1995). So conditions were very favorable for the appearance of WWEs.

Table 4 lists the WWEs that occurred during the IOP according to the classification scheme. There were three type NE and C events, two type NW, N, E and SE events, and one

Table II.4. List of WWEs occurring during the TOGA/COARE IOP (November 1992 through February 1993). Quantities are as defined in Section 3.a. Events whose wind measure statistic exceeds $2.5 \infty 10^6$ m are highlighted by bolding.

Region	Date	Maximum point anomaly (ms^{-1})	Duration (days)	Maximum averaged anomaly (ms^{-1})	Wind measure (10^6 m)
N	31 October 1992	12.6	3	4.3	0.8
E	10 November 1992	11.9	4	4.5	1.2
NE	19 November 1992	14.4	4	5.6	1.2
NW	***20 November 1992***	***12.1***	***10***	***4.4***	***3.0***
NE	25 November 1992	13.0	3	5.4	0.9
E	29 November 1992	11.5	4	2.8	0.8
N	9 December 1992	15.7	3	3.9	0.8
S	***1 January 1993***	***19.3***	***8.5***	***10.4***	***3.8***
C	***2 January 1993***	***14.8***	***11.5***	***6.4***	***4.2***
SE	***3 January 1993***	***14.0***	***7***	***4.4***	***2.5***
NE	***5 January 1993***	***14.8***	***9.5***	***4.0***	***2.5***
NW	27 January 1993	15.3	4	3.5	0.9
W	29 January 1993	11.3	4.5	3.9	1.3
C	***31 January 1993***	***11.0***	***10***	***5.0***	***2.5***
SE	***6 February 1993***	***15.1***	***12***	***6.2***	***4.0***
C	10 February 1993	9.5	4.5	3.7	1.2

type W and S events during the IOP. Maximum point anomalies are □ 15 ms^{-1} in six events, between 10 and 15 ms^{-1} in nine events and less that 10 ms^{-1} in one event. The maximum averaged anomaly offers another indicator of the overall intensity of the event. By this standard the 1-Jan-1993 type S (10.4 ms^{-1}) and the 2-Jan-1993 type C (6.4 ms^{-1}) events are the most intense of the IOP. The next most intense are the 19-Nov-1992 type NE and the 6-Feb-1993 type SE events. The remaining events have maximum averaged anomalies of 5 ms^{-1} or less.

The final column of Table II.4 lists the wind measure of each event, as defined in Section 3. Three "primary" events have wind measure values near $4x10^6$ m, four "secondary" events have values between $2.5x10^6$ m and $3x10^6$ m, and the rest have values less than or equal to $1.3x10^6$ m. The three primary events are the type S and C events centered on 1 and 2-Jan-1993, and the type SE event centered on 6-Feb-1993. The secondary events are the type NW event centered on 20-Nov.-1992, the type SE event centered on 3-Jan-1993, the type NE event centered on 5-Jan-1993 and the type C event centered on 31-Jan-1993. Late December 1992 and early January 1993 was the period of primary WWE activity according to the wind measure. The next most active period was late January 1993 through early February 1993.

These WWE statistics are consistent with westerly wind periods that have been discussed elsewhere. Eldin *et al*.(1994) reported strong westerly winds and found large eastward surface currents from their ship track along 156°E, during early January 1993 and early February 1993. The large westerly wind activity during early January 1993 and during early February 1993 coincided both times with the passage of the convectively active phase of an ISO (Lin and Johnson 1996; Chen and Houze 1996). Three WWEs seem to be associated with named tropical cyclones: the 31-Oct-1992 type N event (cyclones Dan and Carrie), the 20-Nov-1992 type NW event (cyclone Hunt), the 6-Feb-1993 the SE event (cyclone Mick) (McBride *et al* 1995).

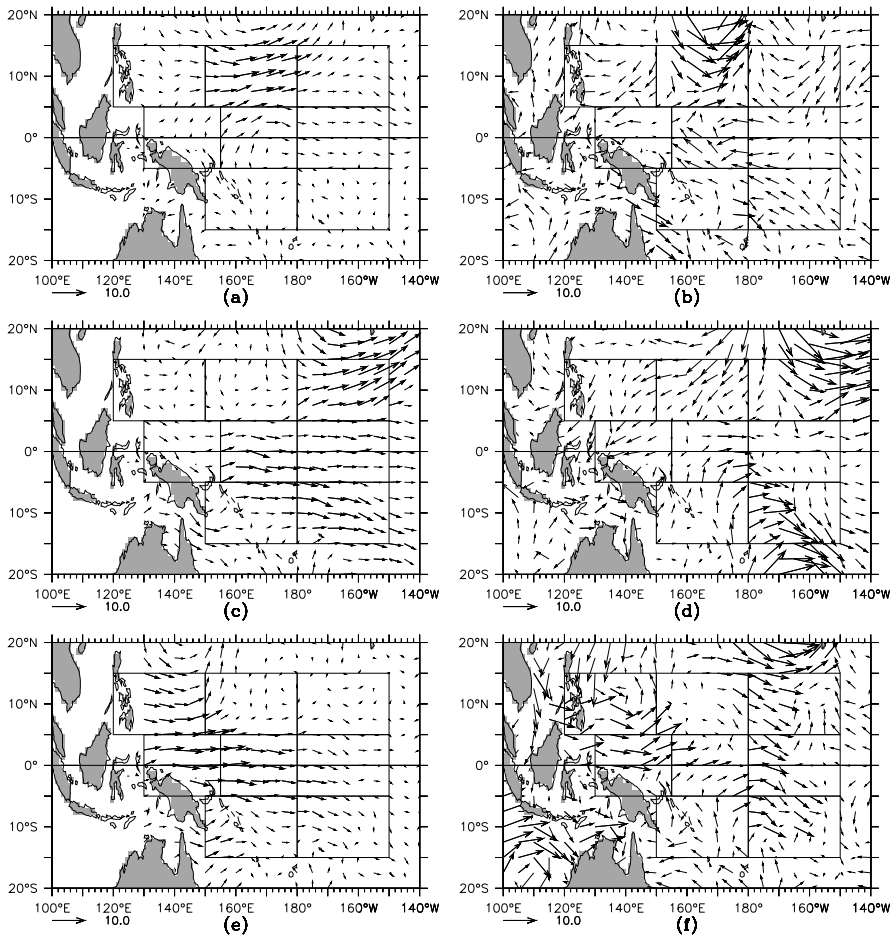

Figure II.20. Vector plots of the wind fields for the composite WWE modeled wind anomaly field on (a) 9 Dec. 1992, (c) 5 Jan. 1993, and (e) 29 Jan. 1993; and ECMWF daily wind anomaly field on (b) 9 Dec. 1992, (d) 5 Jan. 1993, and (f) 29 Jan. 1993. These are three WWE periods occurring during the TOGA/COARE IOP that are well represented by the composite WWE model. Bold wind anomaly vectors indicate zonal wind anomaly exceeding 3 ms^{-1}. Classifying regions are shown by the thin-lined boxes.

How well do the composite WWEs describe the periods of WWEs during the IOP? I have compared the IOP anomaly fields with the wind anomaly fields obtained by simply superimposing the composite anomaly WWEs for the events listed in Table II.4. Vecchi and Harrison (1997) show the results of this comparison for the full IOP period. There are a number of instances in which the simple composite anomaly field is a good first approximation to the real anomaly field, and several instances where the simple field is not so satisfactory. In the interest of brevity I present here only three examples of each. These six event center days are shown for both the modeled anomaly wind field and the daily wind

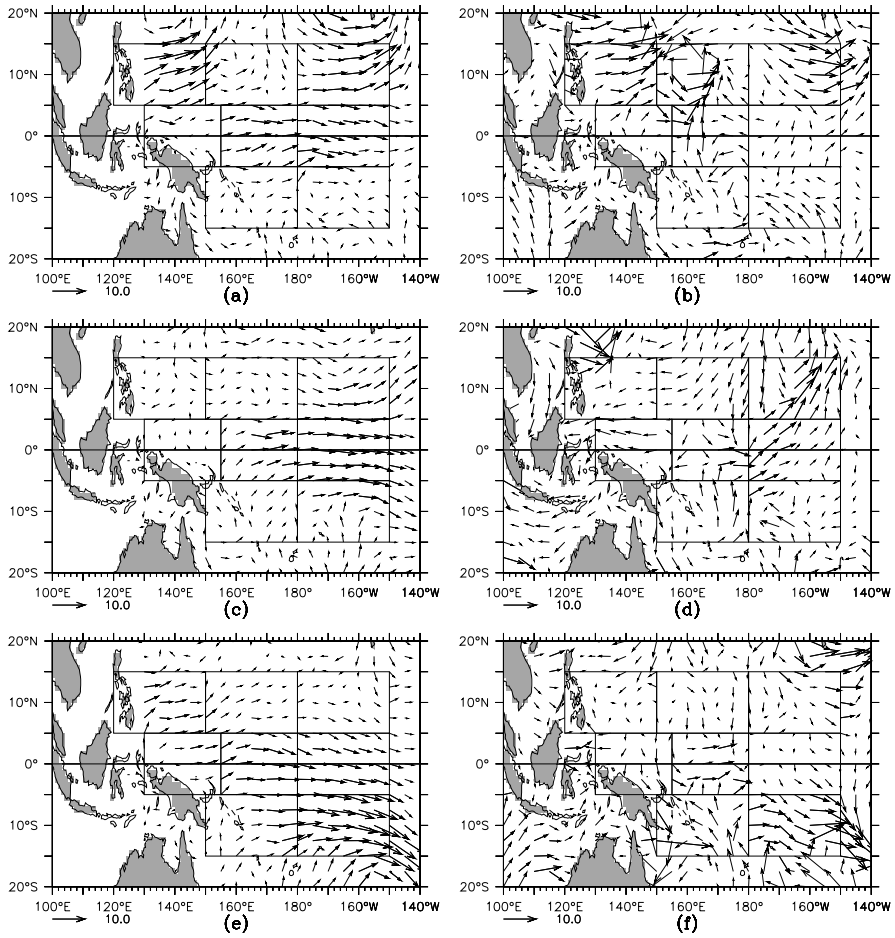

Figure II.21. Same as Figure I.20, except for (a) and (b) 20 Nov. 1992, (c) and (d) 29 Nov. 1992, and (e) and (f) 6 Feb. 1993 These are the three WWE periods occurring during the TOGA/COARE IOP that are most poorly represented by the composite WWE model.

anomaly field, with bold vectors indicating zonal component greater than 3 ms^{-1} (Figures I.20 and .21).

First, consider the three center days when the composite description is a reasonable approximation to the actual anomaly field (9-Dec-92, N; 5-Jan-93, NE and SE; and 29-Jan-93, W and C). Figure II.20 shows that generally the composite description is more diffuse than the daily wind anomaly fields; amplitudes are somewhat reduced and length scales are somewhat larger, even in the defining regions. Outside the defining regions there can be substantial differences, but in these areas the wind anomalies are substantially smaller than in the defining regions.

Now consider the three examples in which the composite fit is least satisfactory (20-

Nov-92, NW and NE; 29-Nov-92, E; 6-Feb-93, SE), shown in Figure II.21. The 29-Nov-92 type E event is quite weak and has substantial (□3ms^{-1}) westerly anomalies only in the western third of the defining region; the composite type E event has westerlies over a much greater zonal extent. This is the only situation in the IOP when the composite does not reproduce the basic features of the wind within the defining region. This is also the weakest event during the IOP, based on the wind measure, and its maximum averaged anomaly is only barely over the identification threshold of 2ms^{-1}. In the other two examples the substantial shortcoming of the composite fit concerns the winds outside the defining regions, particularly near the equator. These IOP off-equatorial events have less equatorial westerly wind than one would expect from the composite WWEs.

More than half the IOP WWEs had a duration shorter than the composite events, so the composite fit produces near equatorial westerly wind anomalies when they were not present in the wind fields. During periods when the WWEs have a duration more like that of the composite events, the fit is much better. This is because while the WWEs identified and averaged to generate the composite WWEs have similar general characteristics, the differences in the details result in a smudged composite WWE.

II.6. Temporal distribution

In this section I describe various temporal relationships for WWEs. I present the climatological distribution of WWEs by month, and define seasonality for each WWE type when applicable. I also show the year to year variation of WWE occurrence and intensity. Finally, I offer some statistics on the extent to which WWEs occur in particular relationships to each other.

a. Single event distributions

Consider first the climatological distribution by month. Figure II.22 shows, for each region, the ten year (1986-95) total number of WWEs that occurred during each calendar

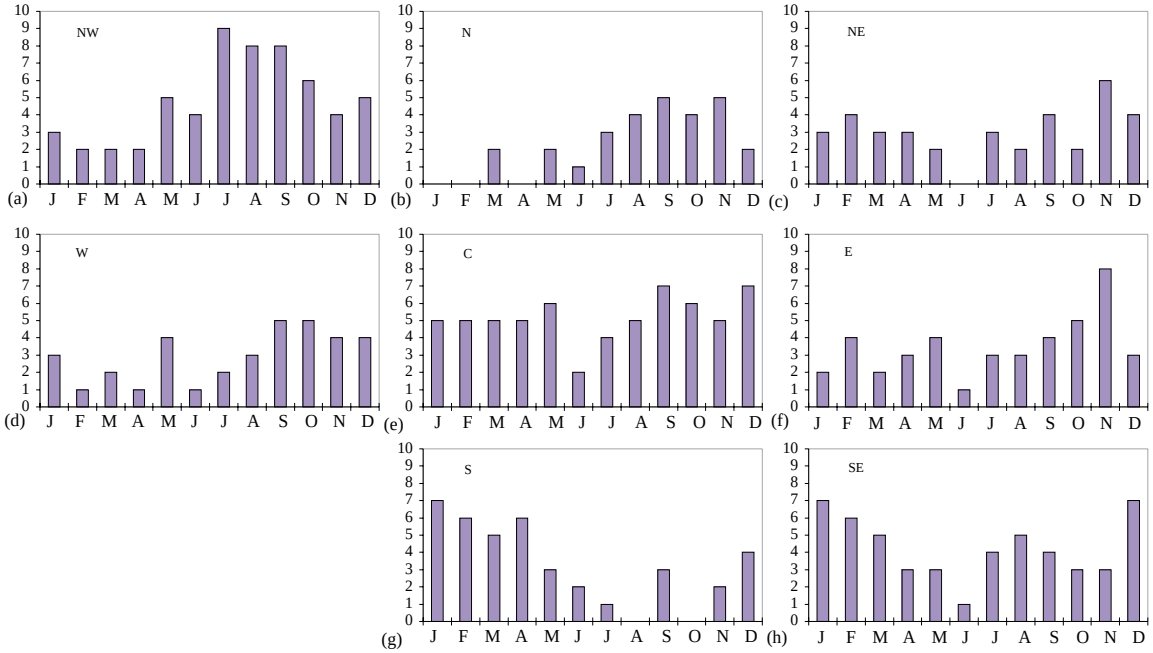

Figure II.22. Monthly distribution of WWEs for type (a) NW, (b) N, (c) NE, (d) W, (e) C, (f) E, (g) S, and (h) SE.

month. No striking variation is seen in the month-by-month comparison, but there is a clear seasonal preference for types NW, N and S, which is statistically significant to the 99% level using the test described in Appendix 1. A seasonal description for the distribution of the type NW WWEs is that of an "on" season from July through October, two transition seasons (May-June and November-December) and an "off" season from January through April. For the type N and S WWEs the simplest seasonal description is that of a six month "on" season, and a six month "off" season. The "on" seasons are July through December for the type N event, and December through May for the type S event. I cannot define an "on" or "off" season for type NE, W, C, E or SE events that is statistically significant at the 90% level.

The distribution of moderate or stronger WWEs is somewhat more striking; defining a moderate or stronger event as an event whose wind measure (see Section II.3.a) exceeds 2×10^6 m, leads to Figure II.23. Boreal summer and fall are the primary seasons for the type NW (July-December) and N (July-October) events; November through January is the primary season for type C events; and boreal winter and spring are the primary seasons for

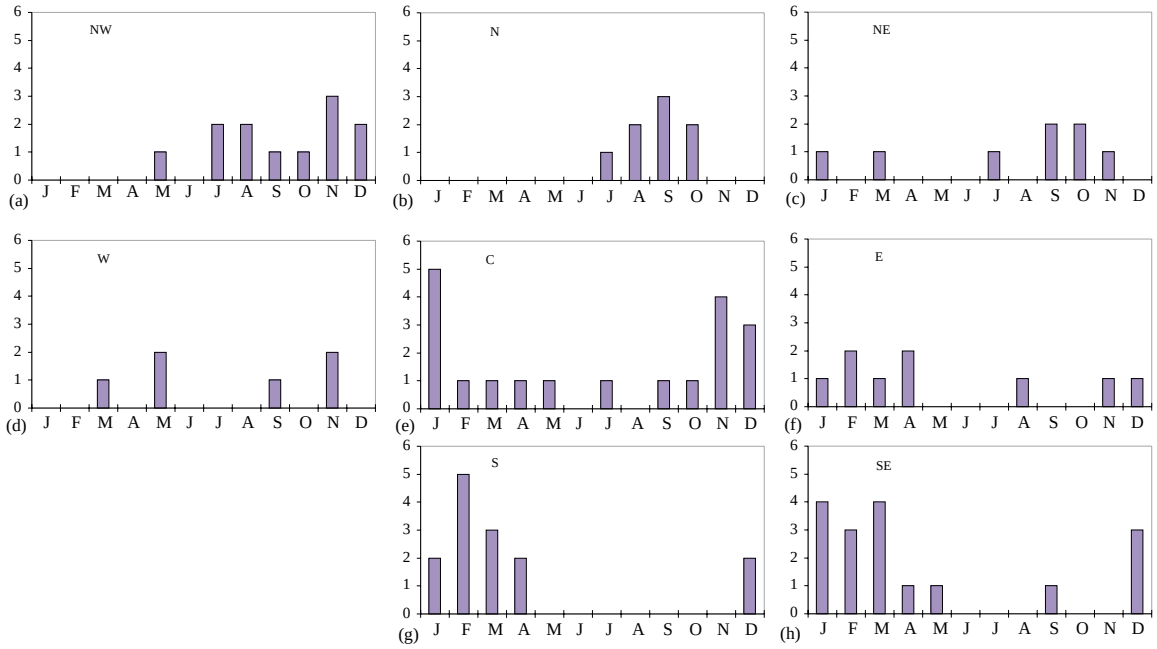

Figure II.23. Monthly distribution of WWEs with mind measure in excess of $2.0 \infty 10^6$ m for type (a) NW, (b) N, (c) NE, (d) W, (e) C, (f) E, (g) S, and (h) SE.

type S (December-April) and SE (December-March) events. While the type C events are evenly distributed across the months, most of the events that occur between November and February are of moderate or greater strength. All these seasonal distributions are significant to the 97% level. No seasonal distribution, significant even at 70%, exists for the strong type NE, W and E events.

Now consider the year-to-year distribution of WWEs. Figure II.24 shows the number of each type event, year by year from 1986 through 1995. The mean number of events is indicated by the thick horizontal line. It is also instructive to compare these distributions with the Troup Southern Oscillation Index (SOI). The twelve month running mean of (-1)xSOI is plotted along with the mean (-1)xSOI for the 10 year period 1986-95, as the lower left hand panel of Figure II.24. SOI values have been negative much of this period, indicating warm (ENSO) conditions for the tropical Pacific; the ten year average is -4.5.

The fewest number of events occurred in 1988 for every type of event, and in most regions 1989 was also a year of few events. 1988-89 was the only period of persistently positive SOI in this record. There is no comparably strong connection between years of

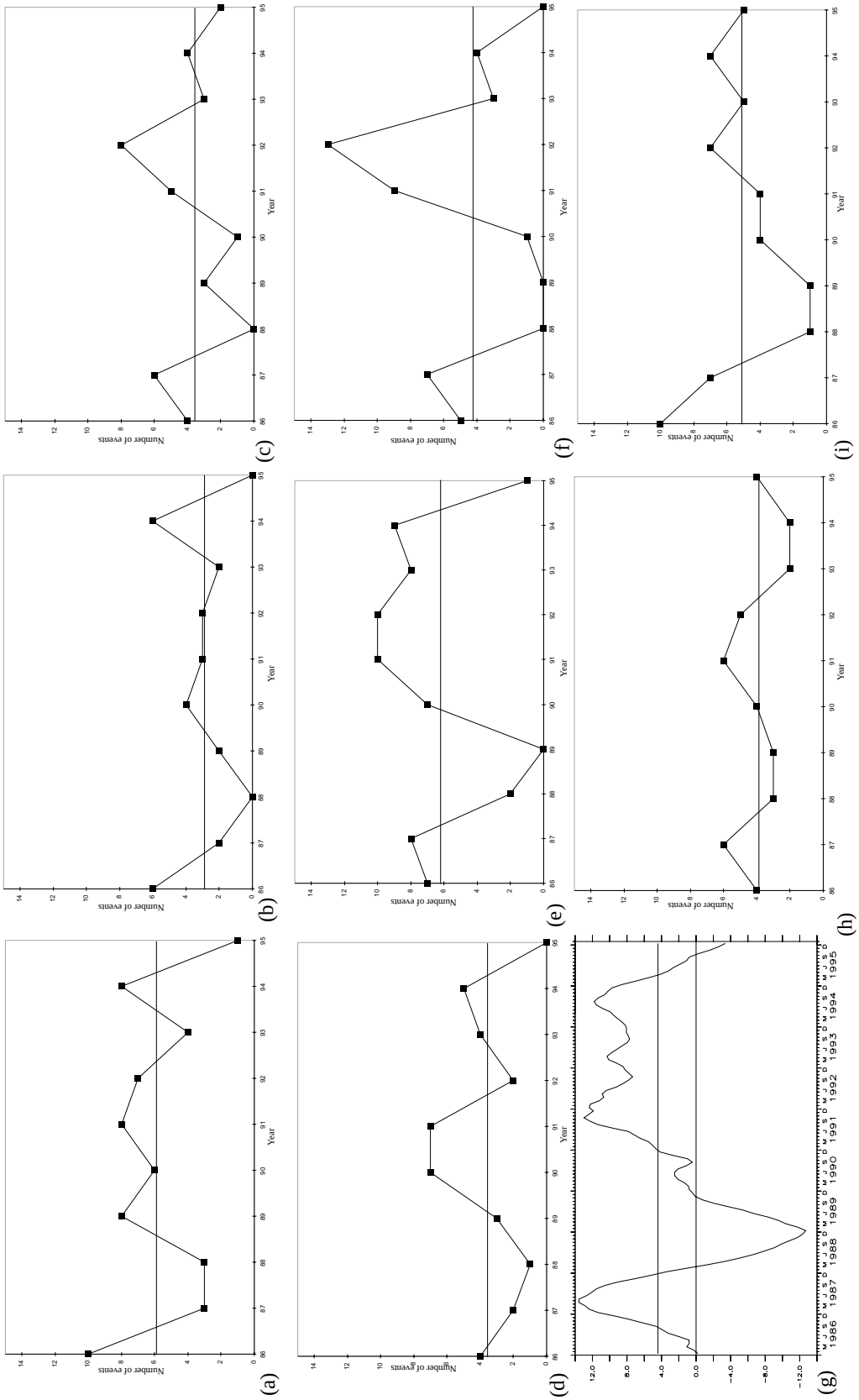

Figure II.24. Plots of yearly distributions of WWEs for type (a) NW, (b) N, (c) NE, (d) W, (e) C, (f) E, (h) S, and (i) SE. Also shown is (g) the 12-month running mean of the quantity (-1)∞Troup SOI Superimposed on all the panels is the 10-yr-(1986-95) mean of each quantity.

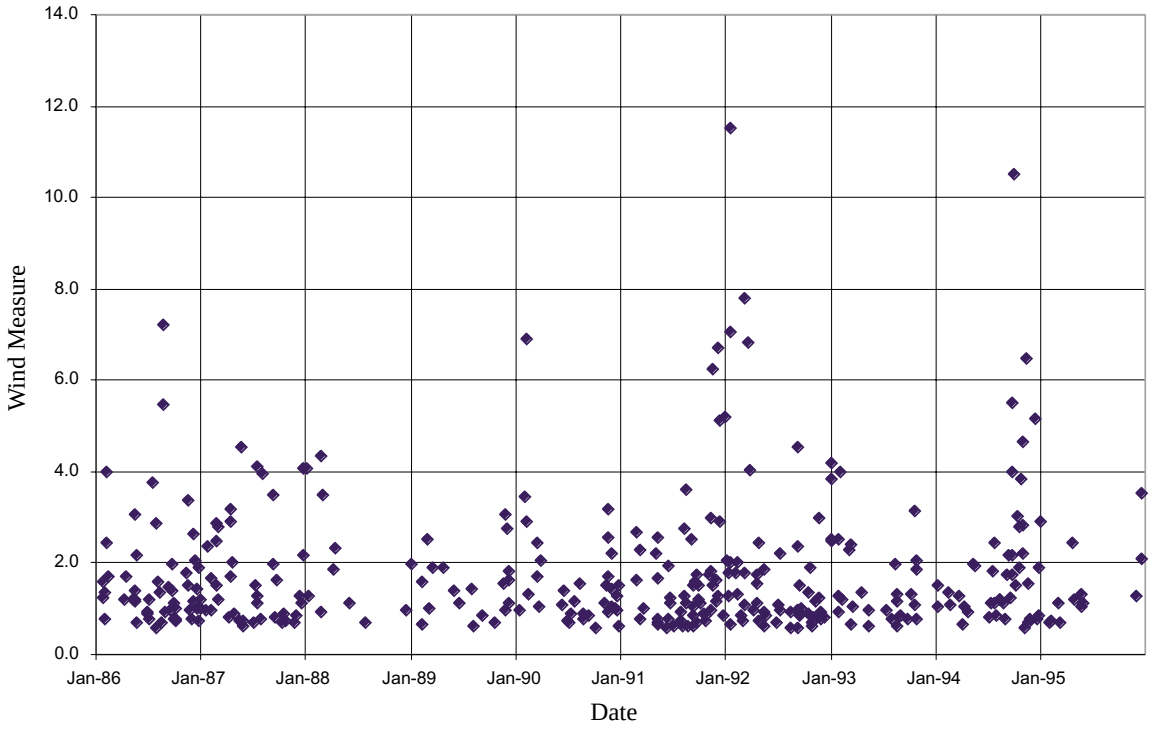

Figure II.25. Scatterplot of wind measure vs. center date of WWE, for all the WWEs in the period 1986-1995. Wind measure is as defined in Section 3.a, and units are 10^6 m.

negative SOI and more than normal total number of WWEs. However lagged correlations between the SOI and the number of events in each region revealed that some statistically significant relationships exist. The strongest correlation (-0.85) exists for type C events at zero lag, and is 99% significant. Zero lag correlations significant at the 95% level exist for type NE(-0.69), E(-0.69) and SE(-0.68) events. Type NW and W regions have 90% significance level correlation (-0.61 and -0.59 respectively) but they lead the SOI by one year. Overall, WWEs in the easternmost three regions and the C region are negatively correlated with zero lag to SOI. WWEs in the westernmost regions are negatively correlated at a one year lead with SOI. Only type N and S events do not show a significant correlation with SOI.

There is another WWE-SOI relationship of interest, which is evident in Figure II.25. In this figure I have plotted a scatter plot of the wind measure of all the events in the10 year record. It is clear that strong events (wind measure > $3x10^6$ m) associate well with periods

of most negative SOI, and that no strong events occur when SOI is positive (see Figure II.24).

b. Multi-event distributions

I have implied an independence of WWEs throughout this study. Typically WWEs form, develop and decay without any strong relationship with other events. I base this on a study of the sequencing of events with center days within three days of each other, looking to determine if there were any statistically significant patterns. In a few instances of substantial statistical significance (99%) different types of WWEs seem to be related. For example, 18% of the time a type N event will evolve into a type NW event (5 times), 17% of the time a type W event will evolve into a type NW event (6 times) and 18% of the time a type S event will evolve into a type SE event (7 times). These three relationships are consistent with the translation speed of the original event. It must be noted that it is not typical for the second event to form out of the first. Two other statistically significant relationships exist in the record, for which I cannot propose mechanisms. In the record 18% of the time a type N event will precede a type SE event (5 times) and 14% of the time a type E event precedes a type NE event (6 times). These last relationships might be coincidental, or there might be some mechanism which accounts for their occurrence. Longer records, containing additional WWEs are needed to determine the robustness of these relationships; only a very few instances exist in the 10-year record.

Another aspect of interest in the frequency distribution of westerly winds was identified by computing the average zonal wind anomaly over the area spanned by all eight of the WWE regions. Recall that a WWE is defined to exist in any one of the WWE regions when the area average zonal wind anomaly exceeds $2ms^{-1}$ for three days. Defining a "Mega"-WWE (MWWE) to exist when the average over all eight regions meets the WWE criterion; there are eleven MWWEs in the analysis period. Figure II.26 provides a cartoon of the spatial structure and wind measure of each MWWE.

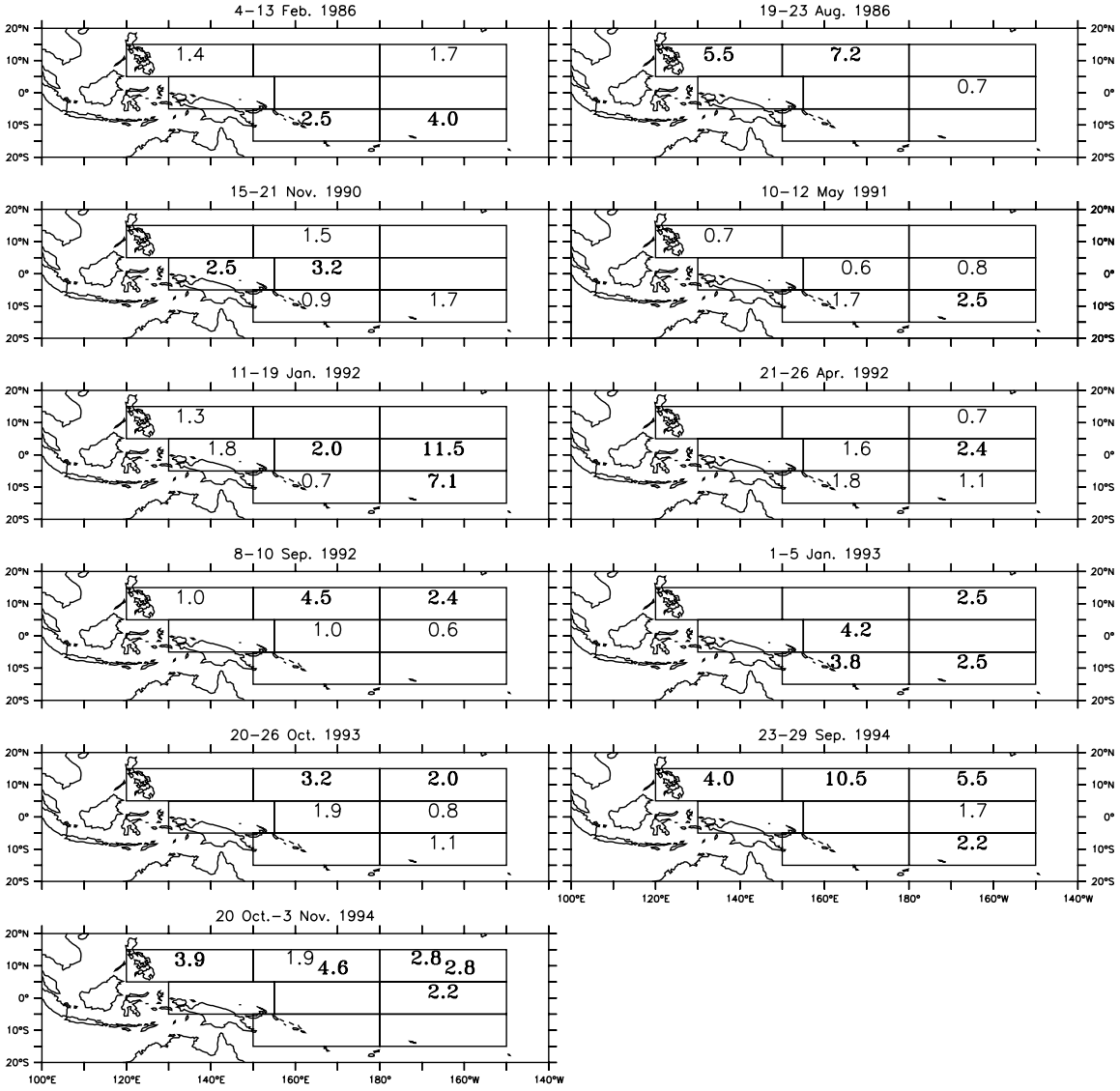

Figure II.26. Cartoon description of the mega-WWEs (MWWEs) in the record. The dates of the MWWEs appear on the top of each figure. Inside the regions involved in the MWWE is listed the wind measure for the particular WWEs. Wind measure values are bolded if greater than $2\infty10^6$ m. Units for wind measure are 10^6 m.

The number of MWWEs by year is: 2-86, 1-90, 1-91, 3-92, 2-93, 2-94; MWWEs only occur during years when the annual average SOI was negative. Of the eleven MWWEs one involves three regions, two involve four regions, six involve five regions and two involve six regions. One MWWE does not involve any of the three equatorial regions, four involve only one, five involve two and one involves all three equatorial regions. In the MWWEs the component WWE of largest wind measure occurs five times in a northern

region, four times in an equatorial region and two times in a southern region. In none of the MWWEs does the W or NW region have the event of largest wind measure. Apart from having events of strongest measure in the central or eastern regions, no clear geographical patterns emerge for MWWEs.

There is a suggestion of seasonality in the meridional frequency of the component WWEs in each MWWE. The five MWWEs for which the dominant component WWEs were northern hemisphere WWEs occurred between the middle of August and the beginning of November; the three MWWEs which had southern hemisphere WWEs as their primary component WWEs all occurred between January and May; the three MWWEs which had equatorial WWEs as their main component WWEs occurred between late November and late April. However there are too few MWWEs for us to do meaningful statistics.

The TOGA COARE IOP contained one MWWE, composed of WWEs with center days between 1-Jan-1993 and 9-Jan-1993. Only this IOP MWWE and one other had each type of WWE in it with wind measure greater than 2.0×10^6 m. Most MWWEs have several types of WWEs with wind measure less than 2.0×10^6 m. The TOGA-COARE IOP thus represented an extreme period of westerly wind variability.

II.7 Summary and discussion

I have examined ECMWF 10m surface wind analyses every 12 hours between 1986 and 1995, to characterize the space and time scales of westerly wind events (WWEs) in the tropical Pacific ocean. I found that Pacific WWEs can be classified satisfactorily according to the region in which they attain their maximum zonal wind anomalies, and that eight adjoining regions are needed to describe the different WWEs in the wind fields. The events are named by the region used to define their existence; regions are named according to their position relative to each other and to the equator (Figures II.5 and II.6): NW, N and NE are

north of the equator; W, C and E straddle the equator; S and SE are south of the equator. With a quantitative measure to define the existence of a WWE, there were 351 events in this period: 58- NW, 28-N, 36-E, 35-W, 62-C, 42-E, 39-S and 51-SE.

I generated a composite event for each type by averaging and find that the zonal wind anomalies associated with each type of event are quite compact in space and time. The structure of each event is modeled as a uniformly translating Gaussian in space and time (Table II.3). The typical amplitude is between 6 and 7 ms^{-1}; the typical *e*-folding time scale is about 3-days (duration is six days between the times of e^{-1} amplitude). The time-scales found by Harrison and Giese (1991) are longer (5-10 days), but the amplitudes obtained in this study compare well to theirs. The meridional *e*-folding scale varies between event types from 400 km to 1,100 km, but values are mostly in the 600-700 km range; these meridional *e*-folding scales are slightly larger to those found by Harrison and Giese (1991). Zonal *e*-folding scales vary from 1,400 km to 2,500 km, while the equatorial events have *e*-folding scales of 1,700 to 1,900 km; Giese and Harrison (1991) estimated a zonal length scale of 20°, that is an *e*-folding scale of about 1,000 km, from the island wind data. Some events translate slowly (largest speed is about 5 ms^{-1}) and others show no significant translational motion. In Section 2 four additional quantities to characterize WWE were defined: duration, maximum point anomaly, maximum averaged anomaly and wind measure; Table II.2 summarizes these characteristics for each type of composite WWE.

This classification method is similar to an extension of that used by Harrison and Giese (1991), except that a two dimensional surface wind field that covers the entire western and central Pacific has been used, instead of a distribution of islands. The analysis can be extended to the zonal scales and translation characteristics of WWEs throughout the entire tropical Pacific. Hartten (1996) used a subjective classification scheme based on the circulation patterns that are observed in association with westerly wind activity, which is defined in terms of wind and not wind anomaly. Hartten's analysis, which covers the area

west of the Dateline, finds many of the circulation patterns seen in the composite WWE analysis; such as cross-equatorial flow, cyclonic circulation patterns and inflow from the west. However, where the trade winds are a strong and persistent feature of the tropical atmospheric circulation, the strong anomalies that are seen in the studies will not usually satisfy her westerly wind burst criterion of 5 ms^{-1} westerly winds. Also, west of the dateline, climatological winds are westerly at 2-3 ms^{-1} in the equatorial western Pacific from November through February, and in the northwestern tropical Pacific (120°E to 145°E, 5-15°N) from July through September. So Hartten's definition identifies as westerly wind bursts situations in which the winds are nearly climatological and does not identify all periods where the wind anomalies are strongly westerly.

Composites like these are most useful when they reasonably well represent the characteristics of typical events in their region. The TOGA-COARE Intensive Observing Period (IOP) provided a four month period (November 1992-March 1993) which contained at least one event of each of the types. The WWEs of the IOP period are summarized in Table II.4. There were 16 WWEs during the IOP; the events with the largest wind measure values occurred late December 1992, early January 1993 and toward the end of January 1993. Another period of strong westerly wind activity was the third week of November 1992. Nine IOP events had wind measure less than $1.3x10^{6}$ m., and seven of the events had wind measure greater than $2.5x10^{6}$ m. Most events had maximum point anomaly values between 11 and 16 ms^{-1}; one event had maximum point anomaly greater than 19 ms^{-1} and one less than 10 ms^{-1}. There was a MWWE in early January 1993, involving four different types of WWEs (S, C, SE and NE) in rapid sequence (center days between 1-Jan-1993 and 5-Jan-1993); this was one of the most intense periods of westerly wind variability in the ten year record. The strong WWEs occurring at the beginning of January 1993 and the beginning of February 1993 were associated with the convectively active phase of an MJO (Lin and Johnson 1996; Chen and Houze 1996). Three WWEs were associated with named tropical

cyclones, two in the northern hemisphere and one in the southern hemisphere

The wind anomaly fields produced simply by superimposing the composite anomalies in place of the particular WWEs of the IOP were compared with the actual wind anomalies. In many cases the composite representation is reasonable. The most common shortcoming is that the weaker WWEs during the IOP typically were of shorter duration than the composites, particularly near the equator. This means that the composite representation tended to have more near-equatorial westerlies than the IOP wind anomalies indicate. It is not simple to characterize the events that are not well modeled by the composites; some had a small wind measure and others a large one, and there were no event types which were dramatically better (or worse) represented by their composite.

Overall, the composite WWEs offer a useful first characterization of the structure of substantial westerly wind anomalies in this region. The composite events are representative of many WWEs, according to the intensity criteria (Figure II.18). However there are events more extreme than the composite events. Because aspects of the oceanic response to WWEs depend on the wind stress or some higher power of the wind stress magnitude, it may turn out that these extreme events must be examined separately in order to understand the full range of ocean response to WWEs. The idealized WWEs used in the response studies of Harrison and Giese (1988) and Giese and Harrison (1991) in their WWE experiments were conservative; indicating that WWEs might force the ocean more strongly than suggested by their idealized experiments.

The distribution of WWEs by year, by climatological month and relative the Troup Southern Oscillation Index (SOI) were also examined. Moderate to strong events (those with wind measure greater than 2×10^6 m) show distinct seasonality for some WWE types (see Section I.6), with off equatorial events tending to favor local summer and fall seasons, and type C events tending to favor boreal winter; while no seasonality is apparent in either the type NE, W or E events. These seasonal distributions are consistent with those found by

Harrison and Giese (1991) and by Hartten (1996). Correlation of annual distribution with SOI is less simply summarized, in part because the SOI was predominantly negative during the period of study - only mid 1988 through mid 1989 and late 1995 had SOI persistently positive. Overall there is a 95% statistically significant negative correlation between SOI and type C, NE, E and SE events at zero lag, and 90% significant negative correlation between SOI and type NW and W events with the events leading the SOI by a year. The type C event is the only event whose correlation with Troup SOI is significant to the 99% level.

The relationships between the existence, preferred location, and intensity of WWEs and the large scale environment of the atmosphere remain to be uncovered. Because the MJO is prominent in tropical convection and free atmosphere zonal wind anomalies (Madden and Julian 1972,1994; Rui and Wang 1990), and because WWEs are often associated with enhanced convection (Kiladis *et al* 1994; Meehl *et al* 1996), a relationship between WWEs and the MJO (particularly the convectively active phase of the MJO) has been suggested (Lau *et al* 1989; Sui and Lau 1992). In particular, the two most intense periods of surface westerly wind variability during the TOGA-COARE IOP occurred in association with the convectively active phase of the MJO. In Chapter IV, I examine the relationships that have been evident in the period 1986-1995 between WWEs, and the MJO and tropical cyclones.

WWEs are an unusual mode of tropical atmospheric variability. According to this analysis the off-equatorial events appear associated with tropical cyclonic systems, but the period in which substantial westerly wind anomalies exist over regions of any significant extent is not characterized by strong translation of the cyclonic system. In this sense, it would seem that these Pacific systems are rather different from their tropical Atlantic counterparts, which usually propagate over large distances once they form. I found nothing similar to WWEs in the ECMWF analyses over the tropical Atlantic or tropical Indian Oceans. In four of the off-equatorial composite WWEs (types NW, N, S and SE) I find moderate (2-

4 ms^{-1}) cross-equatorial inflow and as well as moderate (2-4 ms^{-1}) inflow from the west during the days surrounding the center day (see Section 4.a); Hartten (1996) also has identified cross equatorial circulations into her sort of westerly wind bursts north of the equator, as well as inflow from the west. I are not able to identify a consistent source of alternate-hemispheric flow; the tropical extra-tropical connection remains unclear.

The near-equatorial WWEs are sometimes associated with cyclonic circulations on either (or both) hemisphere. In many instances events of these types appear to be simple down-gradient pressure flows, with meridional scale determined by the atmospheric first radius of deformation. The near equatorial events in the analysis seem also to have a mid-latitude connection, with cross equatorial inflows similar to those described by Love(1985a), Chu(1988), and Chu and Frederick(1990). An interesting feature is the moderate to strong (>2 ms^{-1}) meridional inflow generating poleward of 20° on the days preceding and on the center day of the event (see Section II.4.a).

The near-equatorial events are the primary events to force the ocean east of their location, and it is most likely these events which help to cause warm water to be advected eastward and downward by Kelvin-wave type surges during ENSO events. This type of behavior has been modeled (Schopf and Harrison 1983, Harrison and Schopf 1984, Giese and Harrison 1991) and observed (McPhaden *et al* 1992, Delcroix *et al* 1993) in the equatorial Pacific. Because the SST changes associated with the remote forcing of modest amplitude WWEs is modest - typically 0.5°C over a couple of months, according to Giese and Harrison (1991) - it is not simple to observe clearly in an ocean full of variability on many frequencies. Chapter III deals with the analysis of the SSTA variability associated with each equatorial WWE type, while Chapter V describes the observed eastern Pacific SST warming with an ocean general circulation model (OGCM).